

# FINAL USER BEHAVIOR MODELS AND ABM PLATFORM

SmartH2O algorithms for modelling water customers' behaviours

# **SmartH2O**

Project FP7-ICT-619172

Deliverable D3.4 WP3

Deliverable Version 2.2 – 5 January 2017 Document. ref.: D34.SUPSI.WP3.V2.2 Partners: ...... Coordinator: SUPSI

Contractors: POLIMI,

**Document Number:** .....smarth2o. D34.SUPSI.WP3.V2.2

**Title of Document**: ......Final user behavior models and ABM platform **Author(s)**: .....Alessandro Facchini, Cristina Rottondi, Andrea

Cominola, Matteo Giuliani, Andrea Castelletti, Simona Denaro, Ahmad Alsahaf, Andrea Emilio

Rizzoli.

Approval of this report ......Submitted to the EC for Approval

**Summary of this report:**.....This report presents a set of algorithms to

derive, from metered water consumption data and socio-psychographic features of the consumers, models describing the users' consumption behavior. Specifically, the deliverable reports: two novel algorithms for decomposing high-resolution water flow data into end use categories, the application of several machine learning and data-mining algorithms to the water user modeling problem. The discussed methodologies are validated against datasets available in the literature.

**History**: ......See document history.

Keyword List: .....User behavioural models, user profiling, water

end use disaggregation, agent-based models.

Availability This report is restricted



This work is licensed under a <u>Creative Commons Attribution-NonCommercial-ShareAlike 3.0 Unported License.</u>

This work is partially funded by the EU under grant ICT-FP7-619172

# **Document History**

Version	Date	Reason	Revised by
0.0	19 November 2015	тос	Andrea Cominola
0.1	29 January 2016	Revised TOC after GA	Matteo Giuliani, Alessandro Facchini
0.2	27 February 2016	Section 3 added	Matteo Giuliani, Simona Denaro
0.3	29 February 2016	Section 2 added and 3 completed	Andrea Cominola, Ahmad Alsahaf
0.4	14 March 2016	Section 5, Section 4 and Intro added	Corrado Valeri, Alessandro Facchini
0.5	22 March 2016	Cross-check of sections 1-4-5 + revised introduction	Andrea Cominola, Matteo Giuliani
0.6	23 March 2016	Revised bibliography. Checked Ex. Summary, Sects. 1 and 2. Updated Sect. 4.3.2, created as decided Sect. 4.3.3	Alessandro Facchini
0.7	24 March 2016	Revision	Andrea Castelletti
1.0	31 March 2016	Final Revision	Andrea Rizzoli
2.0	21 November 2016	Following the rewiewers' requests, the profiling of EMIVASA water usage data is added	Andrea Cominola, Matteo Giuliani
2.1	21 November 2016	ABM for EMIVASA case study and update Summary and Intro. Final quality revision.	Alessandro Facchini, Andrea Rizzoli
2.2	5 January 2017	Updates following reviewers' comments. Content reorganised.	A. Facchini, A. Cominola, A. Rizzoli

# Disclaimer

This document contains confidential information in the form of the SmartH2O project findings, work and products and its use is strictly regulated by the SmartH2O Consortium Agreement and by Contract no. FP7- ICT-619172.

Neither the SmartH2O Consortium nor any of its officers, employees or agents shall be responsible or liable in negligence or otherwise howsoever in respect of any inaccuracy or omission herein.

The research leading to these results has received funding from the European Union Seventh Framework Programme (FP7-ICT-2013-11) under grant agreement n° 619172.

The contents of this document are the sole responsibility of the SmartH2O consortium and can in no way be taken to reflect the views of the European Union.





# **Table of Contents**

E	CUTIVE SUMMARY	1
1.	INTRODUCTION	2
2.	END-USE DISAGGREGATION MODELLING	3
:	PROBLEM FORMULATION AND RELATED WORK 2.1.1 Algorithms for water end-use disaggregation 2 SMARTH2O DISAGGREGATION ALGORITHMS 2.2.1 Optimization based algorithm 2.2.2 Hybrid Signature-based Iterative Disaggregation 3 APPLICATION ON REAL-WORLD DATA 2.3.1 High-resolution power load disaggregation 2.3.2 High-resolution water consumption disaggregation 2.3.3 Multi-resolution energy and water consumption disaggregation 3 DISCUSSION AND RECOMMENDATION	3 4 5 5 7 8 8 8 9
3.	SINGLE-USER BEHAVIOURAL MODELLING	17
;	MODEL FORMULATION SMARTH2O ALGORITHMS 3.2.1 Consumption Profiles 3.2.2 Multivariate analysis 3.2.3 Model learning APPLICATIONS TO THE SMARTH2O DATA 3.3.1 Swiss case study - SES 3.3.2 Spanish case study - EMIVASA DISCUSSION AND RECOMMENDATION	17 17 18 19 19 20 20 25 31
4.	AGENT-BASED MODELLING	32
	PROBLEM FORMULATION AND RELATED WORKS SMARTH2O AGENT-BASED MODEL 4.2.1 General SmartH2O agent-based model structure 4.2.2 Portal diffusion model 4.2.3 Behavioural diffusion model B APPLICATION ON SMARTH2O DATA 4.3.1 Modelling observed behavior: Swiss case study - SES 4.3.2 Modelling observed behavior: Spanish case study - EMIVASA 4.3.3 Modelling future behaviour under pricing policies 4.3.4 Sensitivity analysis of the portal diffusion model 4.3.5 Modelling future behaviour under social norms: Swiss case study 5.5.5 Ad 6.6 Modelling future behaviour under social norms: Spanish case stu 6.7.6 Modelling future behaviour under social norms: Spanish case stu 6.7.7 EMIVASA 6.7 DISCUSSION AND RECOMMENDATION	
5.	REFERENCES	55
	ENDIX: MODEL ENGINEERING	61
	DDULES INTERACTION E LOGIC OF MODULES INTERACTION EPLOYMENT OF THE MODULES	61 62 63

## **Executive Summary**

This document is the deliverable D3.4 of WP3, titled **Final user behaviour models and ABM platform**.

According to the DoW, "it updates deliverables D3.2 and D3.3 with the water district agent-based model in its final setting after proper testing and validation against observational data. The deliverable describes a real time data assimilation module to link the model to the smart meter monitoring system. It also contains the final version of the multi-agent model simulator previously described in D3.3. Finally, the deliverable reports on model testing and validation. It provides recommendations for WP6 on model engineering".

The content of the deliverable is organised as follows:

- Section 1 introduces the rationale of the deliverable, which updates deliverables D3.2 and D3.3.
- Section 2 provides an overview on the problem of disaggregation of domestic water consumption data into end-uses and reports the outcomes obtained by testing the two novel disaggregation algorithms described in deliverable D3.2 on water and energy data at different resolutions.
- Section 3 presents the SmartH2O algorithms for modelling single-user consumption behaviours and their application in the Swiss (SES utility) and Spanish (EMIVASA utility) pilot cases.
- Section 4 describes the multi-agent model for predicting household water consumption
  which extends the simulator of deliverable D3.3, and applies it to the two pilot case
  studies of Terre di Pedemonte and Valencia.
- In the Appendix we provide recommendations for WP6 on model engineering.

This deliverable D3.4 relates to other deliverables of the same period as follows:

- D4.3 Incentive Models and Algorithms: this deliverable is the in-depth study, design and implementation of incentives for water consumers in the two pilots (Terre di Pedemonte and Valencia). The SmartH2O ABM model is used in WP4 and applied to the design and implementation of the incentive policies. Specifically, results from this deliverable have been used in WP4 to support the design of an incentive system for the pilots. More specifically, the ABM has been used to estimate the behaviour of users exposed to the incentive policies under design, and to assess the impact of incentives on the distribution of rewards and thus on the budget.
- D6.4 Platform Implementation and Integration second prototype: this deliverable is a software package, which contains the implementation of the simulation platform to predict user behaviour under various types of stimuli, from price incentives to increased awareness.
- D7.2 Validation report (SES): This deliverable reports on the deployment of the Smarth2O platform (inclusive of the incentive models) in the two pilots (Terre di Pedemonte and Valencia) and sets the validation approach that will be followed to compute all the project KPIs. The models of users-consumption behaviours described in Section 2 of this deliverable is instrumental to validation discussed in D7.2. Indeed, it is used to compare consumption reduction levels, or behavioural changes, between groups of users, and to relate platform usage to these clusters.

### 1. Introduction

The SmartH2O user modelling efforts aim at making the most of the smart metered water consumption data to construct behavioural models of water utilities customers' consumption habits. This model building process relies on a three-step procedure:

- 1) identification of end-use patterns;
- 2) classification of observed consumption data into users' profiles;
- 3) simulation of observed and future consumption in response to external stimuli, such as prices, incentives, social norms, etc.

The outputs of the three phases are eventually integrated within an agent-based modelling platform for simulating the observed/future consumption behaviours of the entire community of users served by a water utility. This instrument has the potential for supporting water utilities in designing proper water demand management strategies as it allows predicting their effects on the users' consumption behaviours.

In this deliverable, we report the final results of the activities carried out in Work Package 3. The deliverable updates previous deliverables (i.e., D3.1-D3.2-D3.3) and describes the final setting of the algorithms developed for the construction of the user behavioural models as well as the implementation of the ABM platform.

Section 2 introduces the two SmartH2O disaggregation algorithms developed for the estimation of the **end-use patterns**, the first based on sparse optimization [Piga et al., 2015] and the second one based on a combination of Factorial Hidden Markov Models and iterative Dynamic Time Warping [Cominola et al., 2017]. Both the algorithms are demonstrated to outperform state-of-the-art disaggregation algorithms on power consumption data and to perform satisfactorily also on high resolution water consumption data (numerical results were discussed in deliverable D3.2). The potential for using these algorithms on water consumption data registered at middle/low resolution (e.g., hourly resolution as in SmartH2O pilot applications) is also discussed.

Section 3 illustrates the SmartH2O algorithms for modelling single-user consumption behaviours and classifying them into **users' profiles**. These algorithms combine advanced data analytics and machine learning techniques with a twofold goal: firstly, to describe observed consumption and identify consumption profiles trough a hierarchical clustering procedure; secondly, to identify the most relevant determinants of the observed consumption from a set of candidate variables, including households' characteristics and psychographic features of the users, through feature extraction and feature selection methods [Cominola et al., 2015b].

Section 4 describes both the **social interaction model** and the **response to external stimuli** one, which is based on the Bass/SIRS technological diffusion model coupled with a Young opinion diffusion model. Moreover, it illustrates how the latter can be integrated with the outputs produced by the disaggregation and users profiling algorithms in order to feed the SmartH2O ABM platform.

Finally, Section 5 provides recommendation of how the developed models can be integrated into the SmartH2O platform.

The deliverable also reports the testing and validation of the developed user behavioural models and ABM platform against observational data from the SmartH2O pilot applications. In particular, in this deliverable we present and discuss the results, namely the ABM platform connected to the user behavioural models, for the Terre di Pedemonte (SES utility) and Valencia (EMIVASA utility) pilot applications.

More extensive testing and validation of the developed models will be performed until the end of the project in parallel with the release of the platform. The new results will be included in the deliverable D7.3 "Final overall validation and impact report".

# 2. End-use disaggregation modelling

This section provides an overview on the problem of disaggregation of domestic water consumption data into end-uses and reports the outcomes obtained by testing the two novel disaggregation algorithms described in deliverable D3.2 on multi-resolution water and energy data. Based on these outcomes, the ultimate goal of this section is providing recommendations regarding the impact of data resolution on end-use disaggregation capabilities and the usability of the disaggregation techniques proposed on water data. The Section is organised as follows: the formalization of the problem of data disaggregation and a critical overview of the state-of-the-art techniques to deal with it are introduced in Section 2.1, the SmartH2O disaggregation algorithms based on optimization, machine learning and pattern matching are described in Section 2.2, and their application on water and energy data in Section 2.3. Finally, the outcomes obtained are discussed in Section 2.4, opening up opportunities for useful recommendations on data resolution and end-use disaggregation developments.

#### 2.1 Problem formulation and related work

Recalling the problem formulation presented in Section 3.1 of deliverable D3.2, the problem of disaggregating the measured trace of total water consumption into its end-use components can be classified as a *blind identification* problem [Abed-Meraim et al., 1997] where, given the observed output of the whole system (i.e., the household total water consumption), the unobserved sub-states (i.e., the water consumption of each appliance) are estimated. More formally, considering a house with N different water-using appliances/fixtures ( $L_1, \ldots, L_N$ ) available, we can write its total water consumption  $\overline{Y}$  for each time step t as measured by a single-point smart meter as:

$$\overline{Y}(t) = \sum_{i}^{N} y_{i}(t) + e(t)$$

where  $y_i(t)$  is the consumption of appliance i at each time step t, N the total number of appliances, and e(t) the measure error. Assuming that each appliance  $L_i$  has  $C_i$  operating modes, the consumption of the i-th appliance is written, for each time step, as:

$$\begin{aligned} y_i(t) &= \pmb{B}_i x_i^T(t) + e_i(t) & y_i(t) \in R^+ \\ \pmb{B}_i &= \left[b_{i,1}, b_{i,2}, \dots, b_{i,C_i}\right], & \pmb{x}_i(t) &= \left[x_{i,1}(t), x_{i,2}(t), \dots, x_{i,C_i}(t)\right] & i &= 1, \dots, N \end{aligned}$$
 where:

- $B_i$  is a vector containing the water consumption basis for each appliance i, i.e., the water demand related to each operating state j (e.g., active/not active) of the appliance.  $C_i$  is the number of potential power states of appliance i;
- $x_i(t)$  represents the activation vector for the states of appliance i, at time t. It is binary because it indicates which water consumption basis of vector  $\mathbf{B}_i$  is operating for appliance i, at time t, therefore  $x_{i,j}(t) \in \{0,1\} \ \forall i,j,t$ . Also, each appliance can only operate in one state at a time, thus the following equality constraint holds:  $\sum_{i=1}^{c_i} x_{i,j}(t) = 1 \ \forall i,t$ ;
- $e_i(t)$  is the noise affecting the consumption of appliance i at time step t.

Given a sequence  $D_{T_V}$  of  $T_V$  observations of the aggregate water consumption readings  $\overline{Y}(t)$  (with  $t=1,\ldots,T_V$ ), our goal is to reconstruct the actual water consumptions  $y_i(t)$  (with  $t=1,\ldots,T_V$ ) of each appliance/fixture based on the household aggregate water flow data  $D_{T_V}$ . A training dataset  $D_{T_E}$  is assumed to be available. The training set consists of the observations of the water consumption profiles of each appliance/fixture available in the house. An intrusive period is needed to construct the set  $D_{T_E}$ . During this period, the patterns of the water consumption of each appliance are observed, and information on time-of-day probability characterising the usage of each appliance/fixture can be also gathered.

#### 2.1.1 Algorithms for water end-use disaggregation

The problem of decomposing the aggregate household consumption data collected from a single measurement point into device-level consumption data has been largely studied in the energy sector, prior to the water sector, where also their economic advantages in terms of potentially avoided energy generation and distribution have been demonstrated [Armel et al., 2013]. This brought to the development of automatic disaggregation methods, also known as Non Intrusive Load Monitoring (NILM) algorithms (for a review see [Zoha et al., 2012]).

In the water research literature, several studies have been conducted in the last two decades using a variety of single or mixed disaggregation methods, such as household auditing, diaries, high resolution flow meters and pressure sensors (for a complete review see [Cominola et al., 2015a] and Section 2.1 in deliverable D3.2). According to the methodology adopted, we can identify two main approaches for disaggregating smart metered water data at very high temporal resolution: *decision tree algorithms*, namely Trace Wizard® [DeOreo et al., 1996] and Identiflow® [Kowalski et al., 2003], and *machine learning algorithms*, namely HydroSense [Froehlich et al., 2011] and the approach used in the SEQREUS project [Nguyen et al., 2013]. Recently, the disaggregation of medium resolution water data (i.e., hourly data) has been explored by means of water use signature patterns method [Cardell-Oliver, 2013a,b], namely a combination of feature selection, unsupervised learning, and cluster evaluation.

#### Trace Wizard

Trace Wizard [DeOreo et al., 1996] is a commercial software (recently replaced by an ondemand service developed and managed by Aquacraft Inc) which applies a decision tree algorithm to interpret magnetic metered flow data based on some basic flow boundary conditions (e.g., minimum/maximum volume, peak flow rate, duration range, etc.). The disaggregation requires to (i) conduct a detailed water device stock inventory audit for each household to determine the efficiency rating of each household appliance/fixture, (ii) collect a diary of water use events over a one-week period to gain information on each household water use habits, (iii) create specific templates that serve to match water end-use patterns depending on some basic flow boundary conditions, using water audits, diaries, and sample flow traces and, based on the developed templates, stock survey audit, diary information and analysts' experience, (iv) disaggregate the individual water end-uses. It is worth noting that the human resource effort required by Trace Wizard makes the overall process extremely time and resource intensive, with the quality of the results that is strongly dependent on the experience of the analyst in understanding flow signatures. It has been estimated that the classification of two weeks of data approximatively requires two hours of works by the analyst and attains an average classification accuracy of 70% (Nguyen et al., 2013). In addition, the prediction accuracy of Trace Wizard is significantly reduced when more than two events occur concurrently [Mayer et al., 1999]. However, Trace Wizard still has an edge on disaggregation techniques and has been used in several research works and projects [DeOreo et al., 1994; Mayer et al., 1995; DeOreo et al., 1996; Mayer et al., 1999; DeOreo and Mayer, 2000; Loh et al., 2003; Mayer et al., 2004; Roberts, 2005; Heinrich, 2007; Mead et al., 2009; Willis et al., 2009a, b; Aquacraft Inc, 2011; DeOreo et al., 2011].

#### Identiflow

Similar to Trace Wizard, Identiflow [Kowalski et al., 2003] relies on a decision tree algorithm to perform a semi-automatic disaggregation of the total water consumption at the household level. Identiflow uses fixed physical features of various water-use devices (e.g., volume, flow rate, duration, etc.) to classify the different end-use events. Although Identiflow has shown better performance than Trace Wizard [Nguyen et al., 2013], its classification accuracy strongly depends on the physical features used to describe each fixture/appliance. Two different water events are likely classified into the same category if they exhibit similar physical characteristics.

#### **HydroSense**

HydroSense [Froehlich et al., 2011] is a probabilistic-based classification approach which relies on data collected through pressure sensors. Water end-use events are classified with respect to the unique pressure waves that propagate to the sensors when valves are opened or closed.

Based on the pressure wave, water end-use events are classified by using advanced pattern matching algorithms and Bayesian probabilistic models. HydroSense has been demonstrated to attain very high levels of classification accuracy, namely 90% and 94% with one or two pressure sensors, respectively [Froehlich et al., 2011]. However, the calibration of the algorithm requires an intrusive monitoring period with the installation of a much larger number of pressure sensors connected to each water device (i.e., [Froehlich et al., 2011] used 33 sensors in a single household). This requirement significantly constrains the portability of this approach to a wide urban context as it would entail large costs and privacy issues.

#### SEQREUS approach

The approach used in the SEQREUS project [Nguyen et al., 2013] proposes a combination of Hidden Markov Models (HMMs), Dynamic Time Warping (DTW), and time-of-day probability to automatically categorise the collected data at the household level into particular water end-use categories. To minimise the intrusiveness of the approach, the ground truth for the calibration (i.e., a set of disaggregated end-use events) is obtained using Trace Wizard.

Testing on three independent households located in Melbourne (Australia) demonstrated a high prediction accuracy, namely between 80% and 90% for the major end-use categories [Nguyen et al., 2014]. However, the method still requires human input to achieve such levels of recognition accuracy (e.g., for the classification of inconclusive events supported by DTW and for manually classifying combine events) [Nguyen et al., 2013].

Overall considering the small number of algorithms for disaggregating water flow data, the state of the art literature offers a large room for developing new methods addressing the following major limitations of the existing approaches:

- the requirement of time consuming expert manual processing and intensive human interactions via surveys, audits and water event diaries;
- the usually limited accuracy in identifying overlapping events;
- the challenges posed by the intrusiveness of calibration data acquisition;
- the limited performance in reproducing the timings and frequencies of each device, which would aid the activities of water utilities at different levels, including demand management, network maintenance, and strategic planning.

## 2.2 SmartH2O disaggregation algorithms

#### 2.2.1 Optimization based algorithm

The first water disaggregation algorithm we developed within the SmartH2O is based on sparse optimization, therefore it can be classified as an optimization method, according to the classification proposed by [Zoha et al., 2012] mentioned in the previous section. For an exhaustive description of the features of the algorithm, we refer to [Piga et al., 2015] and Section 3.2 of deliverable D3.2.

In summary, the algorithm we propose here is based on the following two assumptions:

- **A1**: A rough knowledge of the water consumption of each appliance/fixture at each operating mode (i.e., the terms  $B_{i,j}$ ) is supposed to be available. For instance, there terms can be evaluated from the training dataset  $D_{T_E}$  through k-means clustering [Likas et al., 2003].
- **A2**: The water consumption profiles of each appliance/fixture are piecewise constant over time (as it is typical for many residential water-using appliances/fixtures).

Based on the problem definition provided in Section 2.1, the algorithm attempts to estimate the water consumption  $y_i(t)$  of each appliance/fixture at the time sample t by estimation of the time varying variables  $x_{i,j}(t)$  in the following convex optimization problem:

$$\begin{split} \min_{\substack{x_{i}^{(1)}(t),\dots,x_{i}^{(C_{i})}(t)\\t=1,\dots,N\\i=1,\dots,N}} \sum_{t=1}^{T_{V}} \left(y(t) - \sum_{i=1}^{N} \widehat{y_{i}}(t,x_{i})\right)^{2} + \gamma_{1} \sum_{i=1}^{N} \sum_{t=1}^{T_{V}} \left\| \begin{bmatrix} w_{i,1}(t)\\w_{i,2}(t)\\\vdots\\w_{i,C_{i}}(t) \end{bmatrix} * \begin{bmatrix} x_{i,1}(t)\\x_{i,2}(t)\\\vdots\\x_{i,C_{i}}(t) \end{bmatrix} \right\|_{1} + \\ + \gamma_{2} \sum_{i=1}^{N} \sum_{t=2}^{T_{V}} \left\| k_{i} \begin{bmatrix} x_{i,1}(t) - x_{i,1}(t-1)\\x_{i,2}(t) - x_{i,1}(t-1)\\\vdots\\x_{i,C_{i}}(t) - x_{i,C_{i}}(t-1) \end{bmatrix} \right\|_{\infty} \\ s.t. \ x_{i,j}(t) \geq 0, \qquad \sum_{j=1}^{C_{i}} x_{i,j}(t) = 1, \quad i = 1,\dots,N; \quad t = 1,\dots,T_{V} \end{split}$$

In the above formulated problem:

• The first term, i.e.,

$$\min_{\substack{x_i^{(1)}(t),\dots,x_i^{(C_i)}(t)\\t=1,\dots,T_V\\i=1}} \sum_{t=1}^{T_V} (y(t) - \sum_{i=1}^N \widehat{y_i}(t,x_i))^2$$

represents a standard least-square optimization problem. However, it is not sufficient to compute the varying parameters  $x_{i,j}(t)$  by using a simple least-square approach because the problem would be over-parametrised, causing overfitting. This problem is overcome adding the next two terms.

• The second term

$$\gamma_{1} \sum_{i=1}^{N} \sum_{t=1}^{T_{V}} \left\| \begin{bmatrix} w_{i,1}(t) \\ w_{i,2}(t) \\ \vdots \\ w_{i,C_{i}}(t) \end{bmatrix} * \begin{bmatrix} x_{i,1}(t) \\ x_{i,2}(t) \\ \vdots \\ x_{i,C_{i}}(t) \end{bmatrix} \right\|_{1}$$

together with the constraints  $x_{i,j}(t) \geq 0$ ,  $\sum_{j=1}^{c_i} x_{i,j}(t) = 1$ , i = 1, ..., N;  $t = 1, ..., T_V$  regularises the problem by enforcing each appliance to operate at a single mode at each time instant. The 1-norm (i.e., the sum of absolute value of elements of its argument) ensures the problem to be a convex optimization problem, thus it can be solved with through numerical optimisers established in the literature. The parameter  $\gamma_1 \geq 0$  is tuned by the user through cross validation, in order to balance the tradeoff between minimizing the fitting error (by decreasing the value of  $\gamma_1$ ) and minimizing number of the nonzero elements in the vector  $x_{i,j}$ . Finally, the nonnegative weights  $w_{i,j}(t)$  keep into account the time-of-day probability for each end use. For further details on parameters calibration, we refer the reader to Piga et al., 2015.

The third term

$$\gamma_2 \sum_{i=1}^{N} \sum_{t=2}^{T_V} \left\| k_i \begin{bmatrix} x_{i,1}(t) - x_{i,1}(t-1) \\ x_{i,2}(t) - x_{i,1}(t-1) \\ \vdots \\ x_{i,C_i}(t) - x_{i,C_i}(t-1) \end{bmatrix} \right\|_{\alpha}$$

enforces water usage patterns  $\widehat{y_i}(t,x_i)$  to be piecewise constant over time, according to assumption **A2**, and penalises frequent operating state shift.  $\gamma_2$  is a tuning parameter playing a role similar to  $\gamma_1$ . The terms  $k_i$  (with i=1,...,N) are a-priori specified nonnegative weights which can be chosen through the method described in [Piga et al., 2015].

The optimization-based disaggregation algorithm we developed within SmartH2O estimates the time-varying variables  $x_{i,j}(t)$  describing the water consumption of each appliance/fixture by solving the above regularised (convex) optimization problem.

## 2.2.2 Hybrid Signature-based Iterative Disaggregation

In addition to the previously explained optimization-based algorithm, another computationally efficient algorithm for end use disaggregation was developed, as no a priori indications on which category of state-of-the-art literature was identified as best performing. This second algorithm called *Hybrid Signature-based Iterative Disaggregation* (HSID). In principle, it can be classified in the category of supervised learning, pattern recognition algorithms, as it employs pattern recognition techniques to retrieve the temporal structure of consumption trajectories on a training dataset. From another point of view, we can consider the algorithm as a hybrid between supervised and unsupervised methods because, as demonstrated in [Cominola et al., 2017], it is potentially scalable to almost non-intrusive cases, which require a minimum intrusiveness and no fixture-level metering.

The development of HSID is based on the following two assumptions:

- A1: each water consuming device contributing to the total household consumption can be recognised from its specific consumption pattern, i.e., each fixture has a typical signature [Dong et al., 2013; Ruzzelli et al., 2010];
- **A2**: the water consumption level time series of each appliance can be modelled as a Markovian state sequence, and can be represented with a limited number of states (e.g., state 1: fixture operating; state 2: fixture not operating).

For all the details regarding the computations and the implementation of the algorithm, we refer to Section 3.3 of deliverable D3.2 and to [Cominola et al., 2017]. In summary, the HSID algorithm combines Factorial Hidden Markov Models (FHMMs) and Iterative Subsequence Dynamic Time Warping (ISDTW) to accurately characterise end-use trajectories for a number of simultaneously operating appliances and reduce the intrusiveness of the off-line training. More precisely, the operational workflow of the HSID algorithm is composed of the following three steps:

- A. Appliances signatures identification. This first step aims at creating a database containing the signature of each appliance contributing to the total measured consumption at the household level. In order to gather all the needed signatures, the algorithm requires a training dataset  $D_{T_E}$ , consisting of water consumption observations retrieved intrusively for each appliance/fixture during a short training period. The length of the training period should be kept as short as possible, in order to reduce intrusiveness and costs.
- B. 2-state FHMM water consumption disaggregation. The total water consumption trace of each household is partitioned into simplified two-state consumption trajectories for each fixture, in order to identify their operating/non operating states. We used Factorial Hidden Markov Models (FHMMs) for this purpose. FHMMs [Ghahramani and Jordan, 1997] are a well established technique in machine learning and have already been applied in the field of power load disaggregation [Batra et al., 2014]. FHMMs allow the identification of the most probable sequence of states of a Markovian process when the considered system is composed of different sub-components, and the state of the whole system (i.e., the only measured element) is a combination of the hidden states of each sub-component. As an output, FHMMs initially disaggregates the total water consumption signal into 2-state single-appliance piece-wise constant trajectories. Thus, FHMMs provide a rough approximation of the end-use trajectories. As a consequence, the consumption trajectories estimated for each appliance by FHMM assume the shape of piecewise constant lines, i.e., only the operating/non-operating states are detected, while an accurate reproduction of water consumption patterns is missing at this stage.
- C. Trace pattern correction through Iterative Subsequence Dynamic Time Warping. In this phase, we iteratively use Subsequence Dynamic Time Warping [SDTW, Sakoe and Chiba, 1978; Müller, 2007] in HSID to integrate the information on the consumption patterns variety given by the signatures extracted at the beginning of the procedure (Step A), and to correct the 2-state trajectories produced as output in the FHMM step (Step B). The iterative use of ISDTW keeps into account the similarity between the observed total water consumption trace of each consumption event and the signature of each appliance, allowing for a fine correction of the estimated consumption trajectories and the correction of the so-called false detected positive (i.e., appliances modelled as operating in those

time steps in which they are actually non-operating) and false detected negative (i.e., symmetrically, appliances modelled as non-operating in those time steps in which they are actually operating). The correction procedure (detailed in Section 3.3 of deliverable D3.2 and in [Cominola et al., 2017] is iterated in order to correct the signal of all the simultaneously operating appliances, without requiring only one appliance operating at each time step.

## 2.3 Application on real-world data

#### 2.3.1 High-resolution power load disaggregation

Despite the SmartH2O project is focused on the water sector, the two algorithms presented in the previous paragraphs were initially tested and validated against high-resolution, sub-hourly, power consumption data mainly because (i) the state-of-the art literature on data disaggregation is more advanced in the energy sector, thus allowing with a fair comparisons against benchmark algorithms, and (ii) because a dataset of high-resolution residential water consumption data was not available in the initial phases of the project.

More specifically, as detailed in Section 3.4 of deliverable D3.2, the AMPds dataset [Makonin et al., 2013], containing 1-minute resolution power load readings (total household single-point metered power load and single appliance sub-metered power loads) of a single house located in the Vancouver region in British Columbia (Canada), was used to test the two disaggregation algorithms introduced in the previous section.

The results obtained by testing the two algorithms against a set of different performance metrics (see Section 3.5 of deliverable D3.2) show that both the algorithms are able to accurately estimate the fraction of power load consumed by each appliance in the household as well as the sequence of operating states of each appliance and, most importantly, to extract single power consumption profiles for the most contributing appliances. In addition, further research [Piga et al., 2015; Cominola et al., 2017] showed that the application of the two algorithms onto high-resolution data improves and outperforms that of a state-of-the-art 2-state FHMM benchmark algorithm in terms of on/off event detection, precision in the power assignment to the different end-uses, and accuracy in the disaggregated end-uses trajectories. Numerical results also show that the second algorithm, HSID, is robust with respect to noisy training signals and its utilization can be extended to applications that do not require intrusive training periods, ultimately opening up new opportunities to foster the deployment of large-scale high-resolution smart metering networks and the design of personalised demand management strategies.

Yet, after the results obtained on the disaggregation of high-resolution power load data, the real usability of optimization-based and HSID algorithms on SmartH2O data required further testing and investigation because (i) consumption patterns and appliance characteristics of energy-consuming appliances can potentially significantly differ from those of water-consuming appliances, and (ii) water consumption data available from the SmartH2O case studies are collected at 1-hour resolution.

## 2.3.2 High-resolution water consumption disaggregation

A preliminary investigation of the usability of the developed disaggregation algorithms on high-resolution water consumption data was possible only at a second stage of the project, as soon as a dataset containing high-resolution water consumption data for a small set of houses in New Zealand became accessible. The dataset, experiments settings and obtained results are described in Section 3.6 of deliverable D3.2.

In particular, data from a single house metered for 68 days in the period  $27^{th}$  July –  $2^{nd}$  October 2006, and suitable to obtain end-use trajectories at 1-minute sampling resolution, were considered. Both the optimization-based algorithm and the HSID approach were tested and evaluated according to the same performance metrics considered for the previously mentioned electricity experiments.

The main outcome from this first water consumption disaggregation experiments (see details in Section 3.6 of deliverable D3.2) showed that both the optimization-based and HSID algorithms show an acceptable performance in estimating the total contribution of each appliance: the maximum estimation error is around 6%. However, a few drawbacks were noticed if comparing the result with the one obtained for energy disaggregation. The first is that both algorithms managed to estimate the fraction of energy assigned to each appliance with an error lower than 5%, in the applications on energy data. The second is that, even though the consumption share is estimated with an acceptable error, the ranking of actually most consuming appliances is not accurately detected. Finally, performance results in terms of Relative Square Error and R² suggested that the performance significantly decreases in terms of trajectories reproduction accuracy, if compared with the values obtained for electric power disaggregation.

Despite the overall low quality and limited sample size of the data considered for these preliminary experiments on water end-use disaggregation, the outcomes obtained suggested that water end-use disaggregation presents some additional challenges if compared to energy disaggregation, even when considering high-resolution data:

- All appliances operate in a narrow and similar range (in absolute values, the operating range here is 0-30 litres/minute, while energy appliances operated between 0 and few thousand kWh), which already represents a significant limit to appliance identification.
- Some appliances, like tap and toilet show an irregular pattern and operate exactly in the same range, making it hard to identify their consumption patterns and operational states. As such water consumption trajectories do not present a clear signature, the HSID algorithm is likely to be not much effective in correcting the FHMM results.
- Water consumption trajectories for tap and toilet events do not satisfy Assumption A2 in Section 2.2.1. In fact, the disaggregated signals are not piecewise constant over a discrete-time scale with sampling time equal to 1 minute. This is the reason why the optimization-based algorithm shows poor performance in reconstructing the consumption trajectories for tap and toilet events.

As an overall comment to these preliminary results, it was concluded (see Section 3.6.3 of deliverable D3.2) that our first results on high-resolution water consumption end-use disaggregation looked promising in terms of estimation of end-use contributions to total household consumption, but big improvements and deep further investigation were needed to accurately reproduce end-use consumption trajectories.

#### 2.3.3 Multi-resolution energy and water consumption disaggregation

As mentioned in the previous sections, we performed a series of end-use disaggregation experiments against data with progressively down-sampled resolutions, in order to assess the effect of smart meter data sampling resolution on end-use disaggregation capabilities and accuracy and, ultimately, understand possibilities for an actual usability of the disaggregation algorithms we developed on SmartH2O water consumption data, having the latter a sampling resolution of 1 hour. Coherently to the experiments on high-resolution data presented in the previous sections, we performed a number of multi-resolution end-use disaggregation test, detailed below, both on electrical power and water consumption data. The motivations behind this choice are similar to the ones we stated for the above presented high-resolution experiments: benchmark works and datasets are available for what regards power load disaggregation, in addition to the fact that the algorithms we developed have been demonstrated to provide accurate end-use estimates with high-resolution power consumption data. Moreover, a comparative analysis of data sampling down-sample on water and energy disaggregation can support the discussion and recommendation on the obtained outcomes.

#### Multi-resolution power load disaggregation

Regarding multi-resolution power load disaggregation, the tests we performed are characterised by the following experimental settings:

- DATASET: coherently with the experiments described in Section 2.3.1, we considered
  the AMPds dataset and, in particular, the power load contributions given by those
  appliances contributing more than 5% of the total power load consumption, i.e., heat
  pump, forced air furnace, clothes dryer, fridge and security/network equipment. We
  considered a consumption period of 45 days during the months November/December
  2012, with 2-week data for calibration and a month of validation. The training dataset
  consists of the trajectories of each end-use and their sum over the training period.
- DOWN-SAMPLING RESOLUTION: we down-sampled the original 1-minute power load trajectories to build trajectories with the following sampling resolutions: 5, 15, 30, 60, 120 minutes.
- END-USE DISAGGREGATION ALGORITHM: we performed end-use disaggregation
  at the different sampling resolutions mentioned above by use of HSID algorithm. We
  only selected this algorithm because the preliminary experiments show its comparable,
  sometimes better performance than the optimization-based algorithm, and its
  computational efficiency.
- PERFORMANCE EVALUATION: the same performance metrics defined in [Cominola et al., 2017], i.e., *F-score*, *Power contribution error*, and *R2* score are considered. The groundtruth benchmark for performance assessment is the validation dataset sampled for each single appliance at 1-minute resolution.

Performance metrics obtained for HSID on multi-resolution power load end-use disaggregation are reported in Table 1, Table 2, and Table 3.

It clearly appears that, for most of the considered appliances, F-score and R2 quickly decrease for data sampling resolution lower or equal to 5 minutes, also for those appliances that have the largest overall contribution, the biggest operating range and a marked signature, like the heat pump, which is the most contributing appliance and whose groundtruth and estimated trajectories at different resolutions are shown in Figure 1. The only exception holds for the forced air furnace, which keeps a high F-score. However, this is attributable to the fact that it is operating for most of the time, but it is very noisy, as demonstrated by the low R2 and its sudden drop.

Table 1: F-score for HSID applied with different data sampling resolutions.

	1 min	5 min	15 min	30 min	60 min	120 min
Heat pump	0.95	0.80	0.38	0.30	0.25	0.23
Forced air furnace	0.99	0.99	0.99	0.99	0.99	0.99
Clothes dryer	0.80	0.25	0.28	0.11	0.15	0.09
Kitchen fridge	0.95	0.57	0.27	0.49	0.50	0.50
Security/Network equipment	0	0	0	0	0	0

Table 2: Power contribution error for HSID applied with different data sampling resolutions.

	1 min	5 min	15 min	30 min	60 min	120 min
Heat pump	1.3%	2.2%	20.3%	20.8%	21.4%	5.3%
Forced air furnace	1.6%	2.3%	2.1%	1.1%	0.7%	0.007%
Clothes dryer	0.06%	10%	9.6%	5.7%	4.0%	0.6%
Kitchen fridge	0.7%	2.2%	2.8%	0.4%	0.5%	1.4%
Security/Network equipment	1.2%	0.2%	0.03%	0.02%	4e-5%	0.02%

Table 3: R2 for HSID applied with different data sampling resolutions.

	1 min	5 min	15 min	30 min	60 min	120 min
Heat pump	0.98	0.66	0.04	<0	<0	0
Forced air furnace	0.41	<0	<0	<0	<0	<0
Clothes dryer	0.99	0.08	<0	<0	<0	<0
Kitchen fridge	0.77	<0	<0	<0	<0	<0
Security/Network equipment	<0	<0	<0	<0	<0	<0

For all the other appliances, the performance drop is slightly more progressive for the heat pump, because it has a clear signature and operates at high power levels if compared to the other appliances, thus it is easier to identify, while the disaggregation quality sudden drops for the other appliances.

Different comments can be drawn for the *power contribution error* metric, which lowers down for resolutions of 5 to 15 minutes, but then in some cases (e.g., kitchen fridge, clothe dryer) tends to improve again as the resolution lowers down to 120 minutes. Although unexpected, the most likely reason for that improvement is that, with lower resolutions, the estimated signal tends to become closer to a constant signal representing the average end-use consumption over time for the specific appliance (see bottom-right plot in Figure 1).

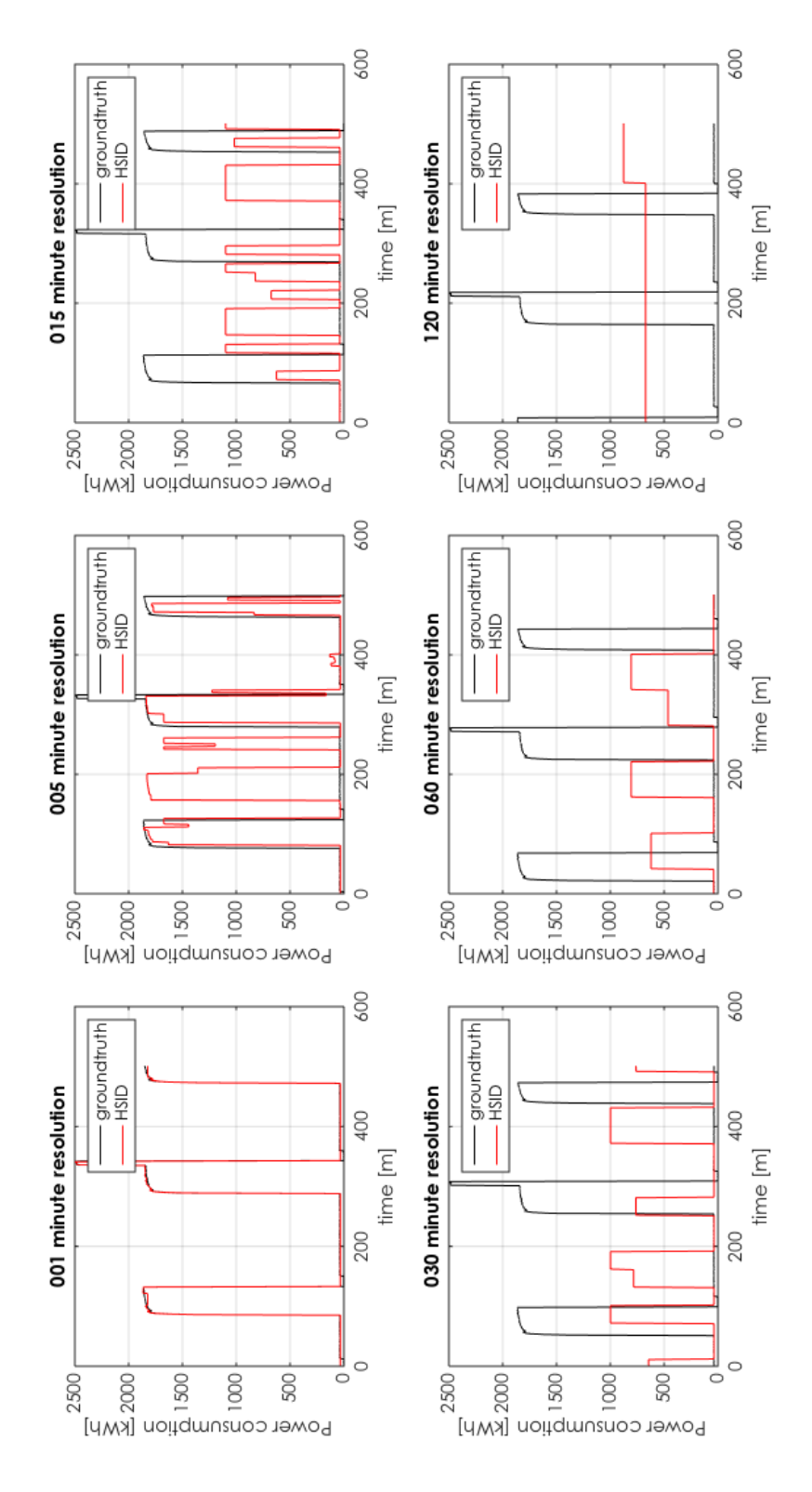


Figure 1: Heat pump groundtruth trajectory (black line) and trajectory estimated by HSID (red line) at different resolutions.

As a consequence, if the training data well represent the average use of a specific appliance, the integral under the estimated power load trajectory over time is likely to be close to the actual consumption of that appliance. Yet, as the power contribution error metric measures the estimate error on the aggregate power consumption, it hides the low accuracy in terms of on/off event detection and accuracy in reproducing the actual consumption trajectories. This represents a strong limitation to disaggregation capabilities at low resolutions. Indeed, even though apparently lower resolution that the minute still allow for an accurate estimate of the overall contribution of each end-use, firstly this accuracy depends on the meaningfulness of the training period, that requires intrusive measurements. Secondly, the outcome of the disaggregation process should be accurate in terms of trajectory estimate accuracy (i.e., Fscore and R2 score) in order to be fully informative to the demand side management. An accurate estimation of the end-use consumption trajectories is essential to provide information on timing of appliance use during the day, peak demands and frequencies of use. The results obtained from the above described experiments suggest that resolutions higher than few minutes strongly affect the ability to retrieve such information. Despite the limited testing does not allow a complete generalization of this evidence, the result obtained is coherent with the work by [Armel et al., 2013], who claim that most of the end uses can accurately be identified with resolutions of 1s-1m, while the number of identifiable appliances strongly reduces and only a very small number of main appliances can be identified at 1-hour resolution by visually observable patterns or correlation with external variables (e.g., temperature), which does not mean they can be accurately disaggregated with automated end-use algorithms.

#### Multi-resolution water consumption disaggregation

Based on the issues raised after the lower performance of our disaggregation algorithms on high-resolution water consumption data, if compared to those obtained for power load disaggregation, and keeping into account that the data collected within the SmartH2O project are sampled at 1-hour resolution, therefore much lower than the 1-minute resolution tested so far, we down-sampled the 1-minute resolution data used for the experiments described in Section 2.3.2 to 1-hour resolution, and repeated the disaggregation experiment. Results from this application, as detailed in Section 3.6.4 of deliverable D3.2 suggested that:

- due to the relatively short event lengths of the considered water appliances, it was not feasible to retrieve the end-use trajectories through disaggregating at this low resolution.
- HSID was found to provide better results in terms of estimating the total contribution of
  each appliance when compared to disaggregating at 1-minute sampled data. However,
  the same consideration does not hold when the optimization-based approach is used,
  thus it appeared that further investigations were needed, to better understand whether
  the improvement in performance of the HSID algorithm were caused by the smoother
  signal created after the 1-hour down-sampling, or by other unknown effects.
- The information on time-of-day probability of the usage of each appliance/fixture cannot be accurately inferred from low-resolution data.

Starting from these preliminary results on a very rough dataset, and adopting the same rationale behind the multi-resolution experiments on power load data described in the previous section, we performed a more rigorous multi-resolution disaggregation by HSID on some synthetically (therefore less noisy) water consumption data. We synthetically generated enduse and total water consumption data, based on end-use duration, volume, frequency, and time-of-use probabilities extracted from the data collected by [DeOreo et al, 2011] from households of various size in nine different cities across the USA [Gaiardelli, 2015] because no sub-hour resolution data are available from the SmartH2O case studies, as well as no enduse groundtruth data,

Coherently to the multi-resolution experiments on energy data, we generated total and enduse water consumption trajectories for 45 days (15 for HSID calibration, 30 for validation), considering end-use probability distributions for a house with 2 occupants. We generated that dataset for five different water consumption fixtures (toilet, shower, faucet, dishwasher, clothes washer) with 1-minute sampling resolution as a baseline and benchmark for validation, and then down-sampled it to 5 and 60 minutes, as 5 minutes sampling resolution resulted to be critical from the previous experiments on power load data and 60 minutes is the resolution water consumption is metered in the SmartH2O case studies.

HSID performances in terms of F-score, Power contribution error and R2 score are summarised in Table 4, Table 5, and Table 6.

In general, already at 1-minute resolution the performance is much lower than the one obtained for disaggregating the same number of appliances considering power load data. We attribute this drop in performance, especially for what concerns operating status detection (F-score) and accuracy in reproducing water consumption trajectories (R2), to the following reasons:

- As Figure 2 shows, if we plot the total water consumption trajectory at 1-minute resolution, the operating range of water consumption appliances is narrow and no clearly identifiable signatures are present. This clearly makes the discrimination among end-uses harder and lowers the effect of HSID signature corrections;
- Again, as it can be seen in Figure 2 and also in [Nguyen et al., 2013], many water
  appliances operate with sub-minute cycles or human-operated events, therefore
  downsampling really makes it hard to distinguish between different appliances (e.g., a
  toilet flush and a short activation of a faucet look similar at the minute resolution and
  their consumption pattern reduces to be one point).

Moreover, the following comments already reported for the electricity case study, are confirmed:

- The accuracy in reproducing the trajectory of the most contributing appliances (i.e., toilet and shower) is slightly higher than that for the other appliances.
- Downsampling from 5-minutes to 60-minutes significantly worsen the disaggregation accuracy.

Table 4: F-score for HSID applied on water consumption data with different data sampling resolutions.

	1 min	5 min	60 min
Toilet	0.46	0.53	0.14
Shower	0.57	0.24	0.07
Faucet	0.44	0.39	0.26
Dishwasher	0.33	0.16	0.05
Clotheswasher	0.22	0.09	0.01

Table 5: Power contribution error for HSID applied on water consumption data with different data sampling resolutions.

	1 min	5 min	60 min
Toilet	3.6%	4.9%	12.6%
Shower	5.8%	4.6%	8.1%
Faucet	2.2%	8.7%	13.1%
Dishwasher	7.8%	5.2%	7%
Clotheswasher	9.6%	0.3%	7%

Table 6: R2 for HSID applied on water consumption data with different data sampling resolutions.

	1 min	5 min	60 min
Toilet	0.20	0.20	0
Shower	0.51	0.03	0
Faucet	<0	0.14	0.07
Dishwasher	<0	<0	<0
Clotheswasher	<0	<0	<0

In accordance to the results shown in the previous section, also in the case of multiresolution water consumption disaggregation the performance in terms of power contribution error remains acceptable even at 1-hour sampling resolution (the maximum error is approximatively 13% on the faucet). However, as mentioned in the previous section, a good performance measured by the power contribution error metric does not reflects into the accuracy in end-use trajectory reproduction, which is needed in order to understand frequencies and appliance time-of-use information, ultimately useful to inform the design of customised water demand management strategies.

In conclusion, the results obtained so far suggest that an accurate end-use disaggregation cannot be performed with the available disaggregation algorithms when the data sampling resolution is lower that a few minutes, or even better, seconds.

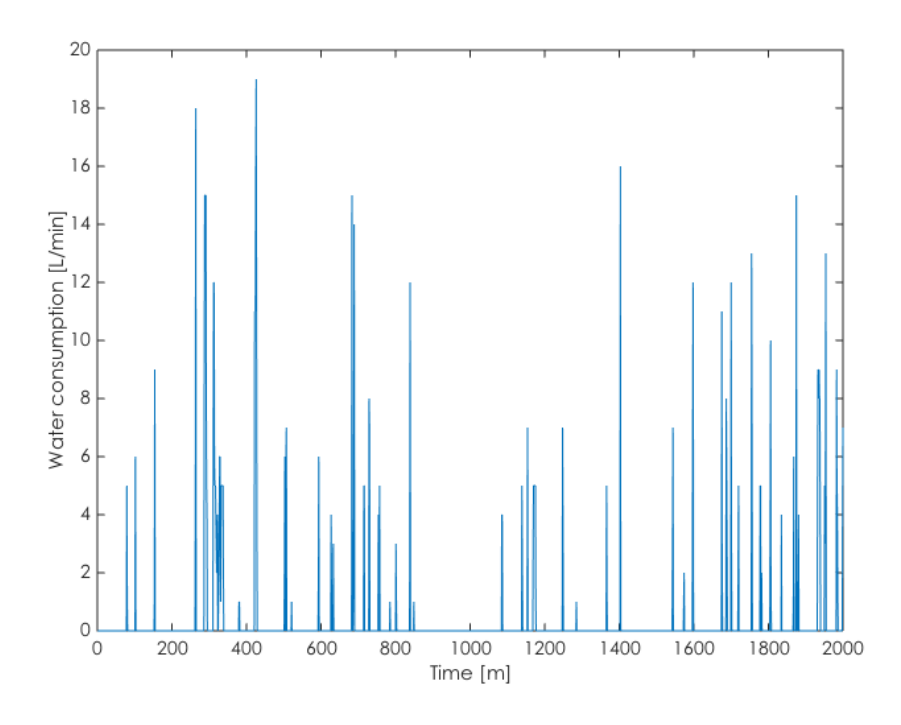


Figure 2: Sample total water consumption trajectory at 1 minute data sampling resolution.

#### 2.4 Discussion and recommendation

In order to explore the possibility to perform water end-use disaggregation, we developed two disaggregation algorithms and tested them on power load and water consumption data at different resolution.

The results obtained for power load disaggregation at high-resolution show that both the algorithms are able to accurately estimate the fraction of energy consumed by each appliance in the household and, most importantly, to extract single power consumption profiles. Moreover, we demonstrated their good performance in comparison to a benchmark state-of-the-art algorithm [Piga et al, 2015; Cominola et al., 2017].

Yet, their performance progressively drops for power load data with lower resolution than 1 minute and significantly lowers when considering water consumption data. The latter are, in fact, characterised by consumption events with shorted duration, often in the order of few seconds or few minutes, and with appliances operating in similar ranges, which makes it harder to extract their consumption pattern from the aggregate, total consumption, signal. This result is coherent with the literature on energy end-use disaggregation [Armel et al, 2013] and with the fact the few works developed in the literature on water end-use disaggregation consider data metered with sub-minute resolution [Nguyen et al., 2013].

The only promising result from the multi-resolution disaggregation on water data suggests that still at low resolution the overall contribution of each end-use and, therefore, the ranking of most consuming fixtures can be retrieved with an acceptable error. However, this would require a suitable and representative calibration dataset, collected intrusively by directly metering each appliance, or with an extensive campaign of water consumption diaries collection.

For the reasons mentioned above and proved by the experimental outcomes obtained so far, an end-use disaggregation of the SmartH2O data, which are sampled at 1-hour resolution and without an intrusively measured end-use groundtruth for calibration, does not appear feasible. However, despite the limited data available for testing, we consider the effort we made in studying the differences in end-use disaggregation between power load and water consumption case studies and the effects of low data resolution on disaggregation capabilities to significantly contribute the field of smart metering and end-use disaggregation development. Firstly, the algorithms we developed contribute improvements with respect to the set of disaggregation algorithms available in the literature. Moreover, the outcomes found in terms of suitable sampling resolution and algorithms development can support water utilities and planners in the choice of suitable meters (i.e., with suitable data sampling), including data sampling resolution as a criterion for the choice, together with data storage and transmission resources and costs.

# 3. Single-user behavioural modelling

#### 3.1 Model formulation

Single-user behavioural models aim at representing the water demand at the household level, thus preserving the heterogeneity of the individual users in the modelled community. In the literature (for a review, see [Cominola et al., 2015a] and references therein), two distinctive approaches exist: **descriptive models**, which are focused on the analysis of observed water consumption patterns, and **predictive models**, which instead provide estimate of the expected water consumption.

Descriptive models aim at studying historical trends [Agudelo-Vera et al., 2014; Kofinas et al., 2014] in order to build consumption profiles that constitute the baseline for identifying the most promising areas where conservation efforts may be polarised (e.g., restriction on irrigation practices in case gardening represents the dominant end-use). Depending on the resolution of the data available, the analysis can focus on identifying aggregated consumption patterns or on defining users' profiles on the basis of the disaggregated end-uses (e.g., [SDU, 2011; SJESD, 2011; Willis et al., 2011; Cardell-Oliver and Peach, 2013; Beal et al., 2014]).

Predictive models aim at estimating the water demand at the individual (household) level, as determined by natural and socio-psychographic factors, or in response to alternative WDMS. The construction of predictive models generally follows a two-steps procedure:

- 1. multivariate analysis, which consists in the identification and selection of the most relevant inputs, such as economic drivers (e.g., [Olmstead et al., 2007; Rosenberg, 2010]), hydroclimatic drivers (e.g., [Balling et al., 2008; Polebitski and Palmer, 2010]), and users' personal attributes (e.g., [Matos et al., 2014; Romano et al., 2014]), to explain the preselected output (i.e., observed consumption patterns).
- 2. model learning, which consists in the identification, calibration, and validation of mathematical models describing the users' behaviours as a function of the drivers identified in the multivariate analysis. In the behavioural modelling literature, we can identify a first class of models, named single-user models, which describe the consumption behaviour of individual users considered as isolated entities. These works (e.g., [Kenney et al., 2008; Maggioni, 2015)] generally rely on dynamic models based on sampling of statistical distributions describing average users and/or end-uses. Water demand patterns can be then estimated via model simulation and comparison of the results with the observed data. A second class of behavioural models, named multi-user models, instead focus on studying the social interactions and influence/mimicking mechanisms among the users.

This Section focuses on the construction of the **SmartH2O** single-user behavioural models, while the multi-users models are described in Section 4.

# 3.2 SmartH2O algorithms

The general procedure for constructing a single-user behavioural model is composed by three main phases:

- 1. identification of **consumption profiles** from the analysis of observed consumption (as in descriptive models);
- 2. **multivariate analysis** for selecting most relevant drivers associated to the identified consumption profiles:
- 3. model learning to describe the average consumption behaviours of single users.

Each step of the procedure requires specific algorithms in order to construct the final single-user behavioural model. This section introduces the algorithms developed within the SmartH2O

project, while their application to the SmartH2O data is reported in Section 3.3.

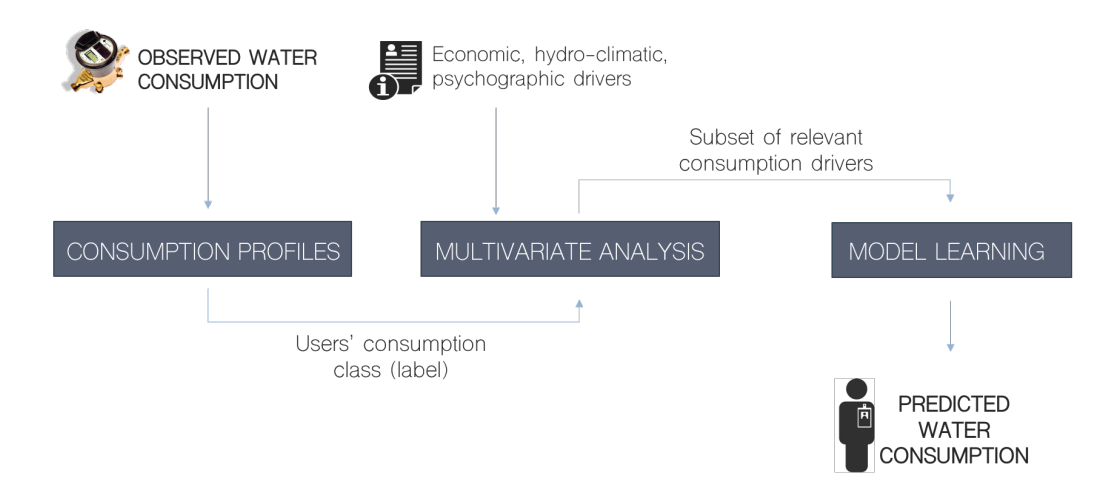


Figure 3: Flowchart of the general procedure for constructing single-user behavioral models.

#### 3.2.1 Consumption Profiles

The identification of the consumption profiles is based on a hierarchical clustering procedure applied on some consumption indexes derived from the observed water consumption data of the single users, which are obtained from the smart-meters network. Our procedure relies on the K-mean clustering method, an iterative algorithm that aims at minimizing an error term based on the distance between each data instance and the K cluster centroids. In particular, we used a variant of the standard K-mean adapted for handling both numeric and categorical variables. The clustering can be performed on a variety of consumption indexes, such as the average consumption in each hour of the day, the average consumption for each day of the week, the average consumption for weekdays or weekends, the average day with the highest consumption within a week, the average period of the day with the highest consumption within the 24 hours, the typical hourly consumption patterns within a day, etc. However, many of these indexes are likely highly correlated and contain redundant information. The most informative subset of indexes for characterising the consumption profiles can be the identified through correlation analysis, feature extraction techniques, and trial and error tests to analyse the redundancy of the indexes, the accuracy of the clustering procedure in terms of cluster silhouette, the separation of the clusters, and the interpretability of the results.

This clustering procedure allows classifying the observed consumption behaviours into different profiles. Then, for each consumption profile, we estimate two probability density functions from the observed consumption data of the users associated with that profile, one for the weekdays and one for the weekends, which allows simulating daily consumption behaviours. Finally, we identify typical sub-daily consumption patterns by means of the **load-shape method** [Kwac et al., 2014], which performs a disaggregation of the simulated daily consumption into higher resolution data through a three-step hierarchical methodology:

- 1. The consumption profile of each day along the water consumption time series sampled for each user is normalised over the total daily consumption over that day in order to define an archive of candidate representative load shapes for the whole consumers' community.
- A set of representative load shapes is selected from the archive created at step 1.
   More specifically, the set of selected load shapes results as output of an adaptive K means clustering algorithm that iteratively splits the load shapes archive until each
   cluster centroids well represents the load shapes belonging to its class in terms of
   centroid distance.

3. The set of representative load shapes is iteratively reduced by merging clusters whose centroids' linear correlation is above a certain threshold (we set such a threshold to 0.5) and redefining new centroids on the merged class as a weighted combination of the centroids of the classes to be merged (we modified this part of the algorithm with respect to the one proposed in [Kwack et al., 2014], in order not to define a priori the number of load shapes to obtain as output). The final set of representative load shapes, which is the output of the model, is constituted by the centroids of the final clusters setting.

Once the set of representative load shapes is evaluated, each user in the considered sample can be matched to his/her most representative load shape (or, more frequently, load shapes, if he/she has a variable behaviour).

#### 3.2.2 Multivariate analysis

A predictive model of the single-user water consumption can be formulated as

$$\widehat{y}_i = f(x_i),$$

where  $\widehat{y}_i$  represents the predicted consumption of the *i*-th user and  $\mathbf{x}_i$  is the set of M drivers influencing his/her behaviour. The union of these drivers and the observed consumption  $y_i$  yields a sample dataset containing N tuples (one for each user) of the form:

$$< x_i^1, x_i^2, ..., x_i^M, y_i >$$

The aim of the multivariate analysis is the identification of the *M* most relevant drivers that allows explaining the observed consumption and, consequently, can be also employed to accurately predict the water consumption behaviours of a user as dependent on his/her drivers. Feature extraction techniques, mostly developed in the data mining and machine learning research communities, represent promising tools to run the multivariate analysis. Different approaches can be adopted to perform feature extraction, which can be classified in two main categories [Galelli et al., 2014]:

- **Feature selection**, namely algorithms that return a subset of features selected from the original dataset as the most relevant to describe the considered output variable (i.e., consumption profile);
- **Feature weighting**, namely algorithms that rank all the features according to a measure of their relevance, with no actual selection of the most relevant variables, which however are identified as the ones in the first positions of the ranking.

Since, a priori no single method is best suited to all datasets and modelling purposes, we implemented and applied different algorithms for both feature selection and weighting. More details about these algorithms can be found in deliverable D3.2 – First User Behaviour Model.

#### 3.2.3 Model learning

In principle, any data-driven modelling approach (regressor or classifiers) can be used in the model learning phase to build a single-user behavioural model (e.g., [Maier and Dandy, 2000; Galelli and Castelletti, 2013]). In practice, the selected method should have the following desirable features: modelling flexibility to approximate strongly non-linear functions, particularly because the relationships between the candidate inputs (selected features) and the output (consumption profile) is completely unknown a priori; computational efficiency to deal with potentially large datasets, when considering large number of users; scalability with respect to the number of candidate variables to be analysed, due to the need of testing several variables with different domains and variability.

The following two data-driven modelling approaches have been tested: **Naive Bayesian Regression** [Duda et al., 1973] and the J48 java implementation of the C4.5 **Decision Tree algorithm** [Quinlan, 1993]. More details about these algorithms can be found in deliverable D3.2 – First User Behaviour Model.

## 3.3 Applications to the SmartH2O data

#### 3.3.1 Swiss case study - SES

The application of the developed algorithms for constructing single-user behavioural models was run on the dataset collected by Società Elettrica Sopracenerina (SES) during the SmartH2O project. The dataset used comprises water consumption readings at 1-hour resolution for 256 users over the time period March 2015 – October 2015<sup>1</sup>. Given the limited length of the dataset, we were not able to include the effect of seasonality in the estimation of the consumption profiles. Moreover, since no psychographic variables of the metered users are available (they are being collected through the SmartH2O platform but, currently, these data do not allow a statistically significant representation of SES customers' population), the construction of the single-user behavioural model is limited to the identification of the consumption profiles, without any multivariate analysis. The simulation of the single-user water consumption is hence obtained by sampling the pdf characterising the identified consumption profiles.

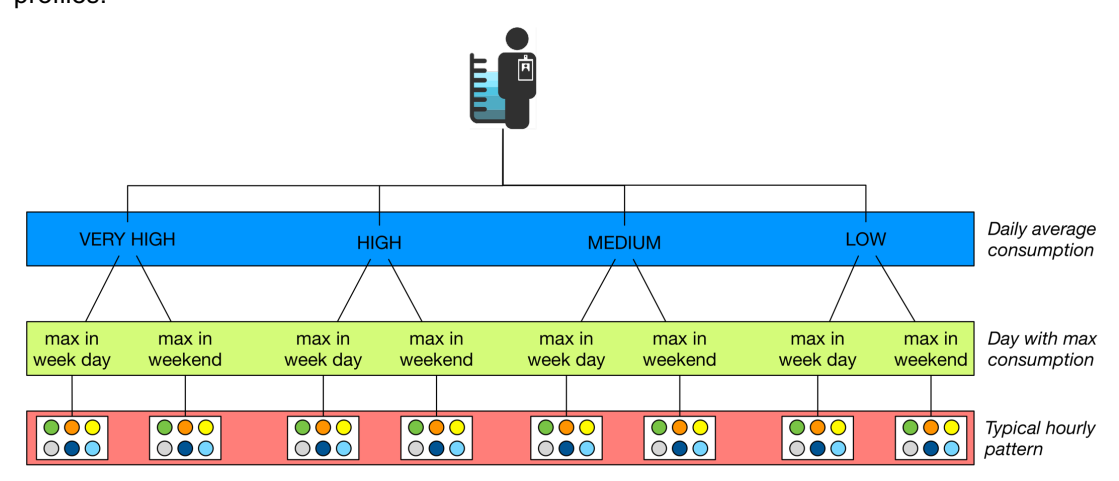


Figure 4: Hierarchical clustering procedure for the identification of the consumption profiles.

The hierarchical clustering procedure adopted for the identification of the consumption profiles of SES users is summarised in Figure 4. We tested more than 40 consumption indexes and, among them, we obtained the best results in terms of clustering accuracy, separation of clusters, and interpretability of results by using the **daily average consumption** combined with a **day-label** identifying if the users has the maximum daily consumption in a week day or during the weekend. In particular, we extracted 4 clusters computed on the average daily consumption and, then, each cluster is partitioned again in two subclasses depending on the day-label. The resulting profiles, illustrated in Figure 5, show a good separation of the clusters and also a good distribution of the users among the profiles, with the medium and low profiles containing more users than the high and very high ones.

Actually, for some users the data are available on a shorter time period depending on the time of installation of the smart-meter.

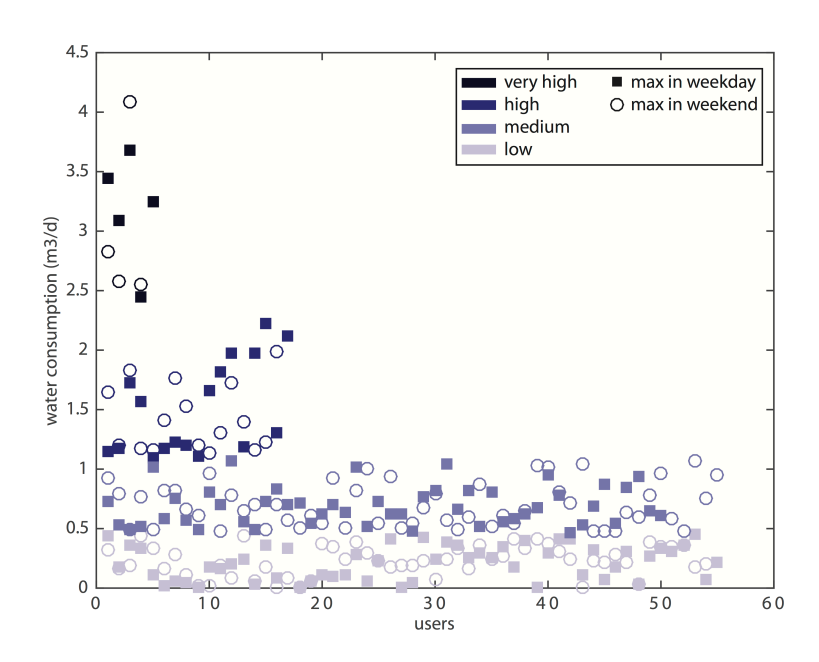


Figure 5: Daily consumption profiles of SES users.

Each profile is then modelled by estimating two probability density functions (assuming a normal distribution), the first for the daily consumption in weekdays and the second for the daily consumption in weekends. The statistics characterising the 8 probability distribution functions are reported in Table 7. It is worth noting that the estimated standard deviations are larger in weekends than in weekdays due to more regular routines of the users during the week. In fact, during weekdays most users are likely to be at work during the central hours of the day and, consequently, their water consumption is concentrated in the morning and in the evening with consumption behaviours repeated almost equally every day at the same time.

Table 7: Statistics associated to the identified consumption profiles. All the values are expressed in m3/d.

Profile	M weekday	Std weekday	M weekend	Std weekend
Very high – max in weekday	3.2330	0.6082	3.0598	1.1171
Very high – max in weekend	2.7278	0.2204	3.7082	2.0043
High – max in weekday	1.5209	0.4322	1.4867	0.3553
High – max in weekend	1.4330	0.3124	1.4183	0.3012
Medium – max in weekday	0.6928	0.1732	0.6877	0.1810
Medium – max in weekend	0.6843	0.1842	0.7271	0.2448
Low – max in weekday	0.2212	0.1450	0.2042	0.1515
Low – max in weekend	0.2267	0.1230	0.2351	0.1413

From this statistical characterisation of the 8 consumption profiles, we finally model the single-user consumption behaviours by sampling the corresponding pdfs to generate a trajectory of daily water consumption for each user. Then, the generated trajectory is disaggregated from daily to hourly resolution by using the most typical load-shapes associated to each user. In total, we have identified 34 load-shapes, reported in Figure 6, which have been grouped into 6 classes on the basis of their similarity in order to characterise typical hourly consumption

patterns: unclassified/zero consumption in green, morning peak in orange, afternoon peak in yellow, evening peak in grey, double peak (one in the morning and one in the late afternoon or evening) in dark blue, multiple peaks in light blue.

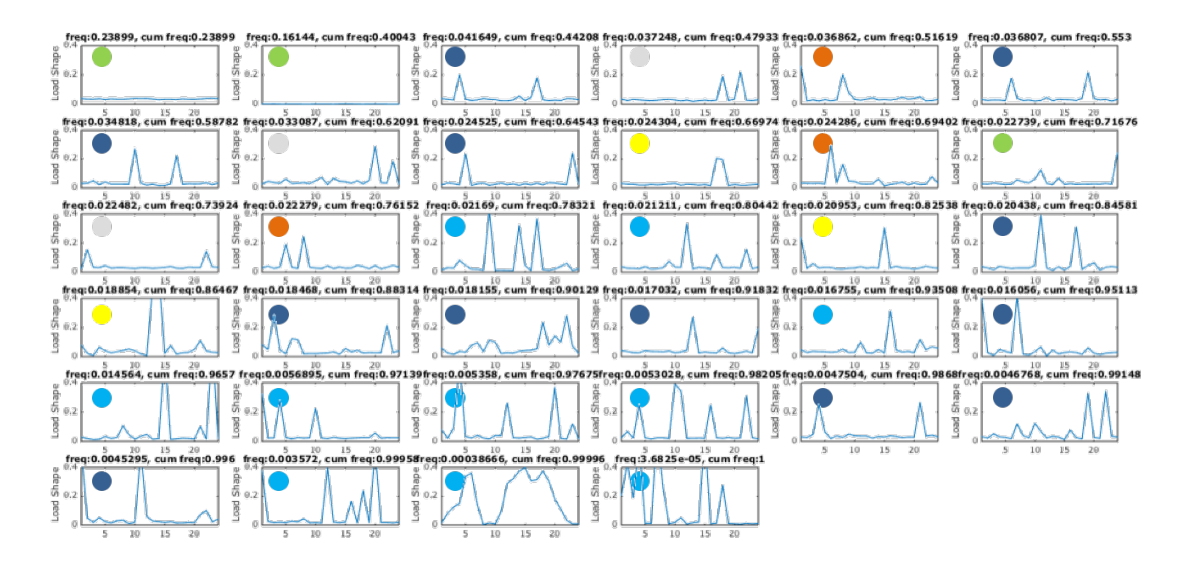


Figure 6: Set of load-shapes representing the typical hourly consumption patterns for SES users.

We evaluate the accuracy of the modelled single-user behaviours by comparing the simulated consumption over 245 days (i.e. March 2015 – October 2015) against the observed one. Figure 7 shows that the distribution of the simulated daily consumption is very close to the observed one, with a small underestimation of the low consumers, which is probably due to the bias in the low consumer class introduced by some metered household that are second houses used only during periods of vacations.

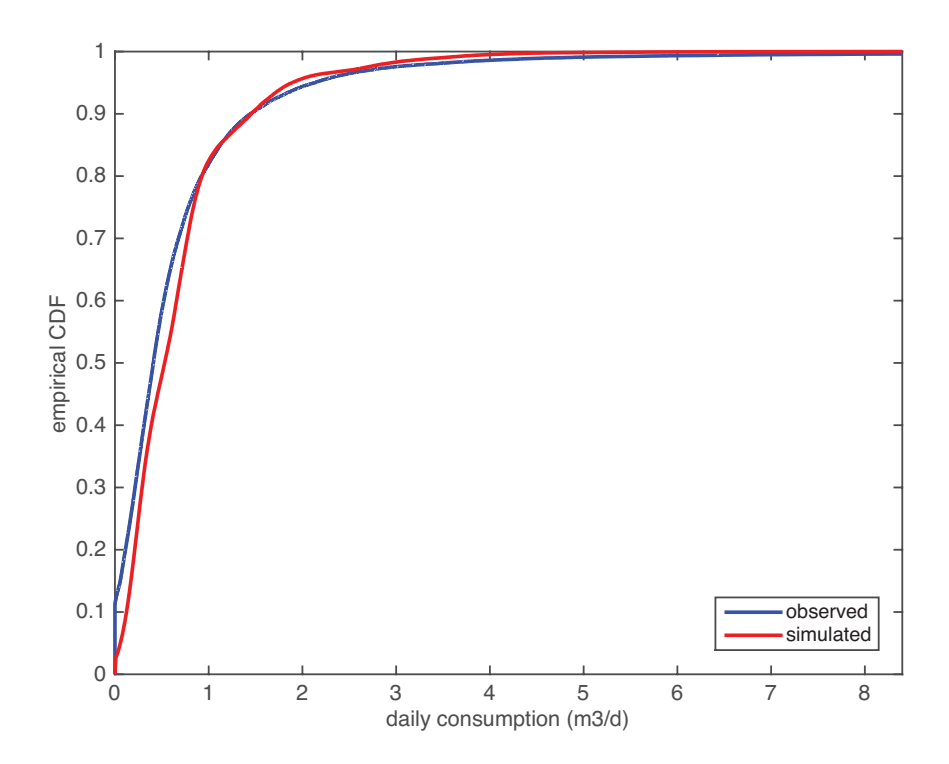


Figure 7: Empirical cumulative density function of daily consumption of SES users.

A more detailed comparison can be performed by comparing the empirical CDFs of simulated and observed consumption separated for weekdays and weekends, see Figure 8. Results show that our profiles successfully capture the differences in the users' behaviours: despite the consumption during the weekend is generally higher than during weekdays (see the x axes of the two panels), both the CDFs computed from simulated consumptions are close to the observed ones.

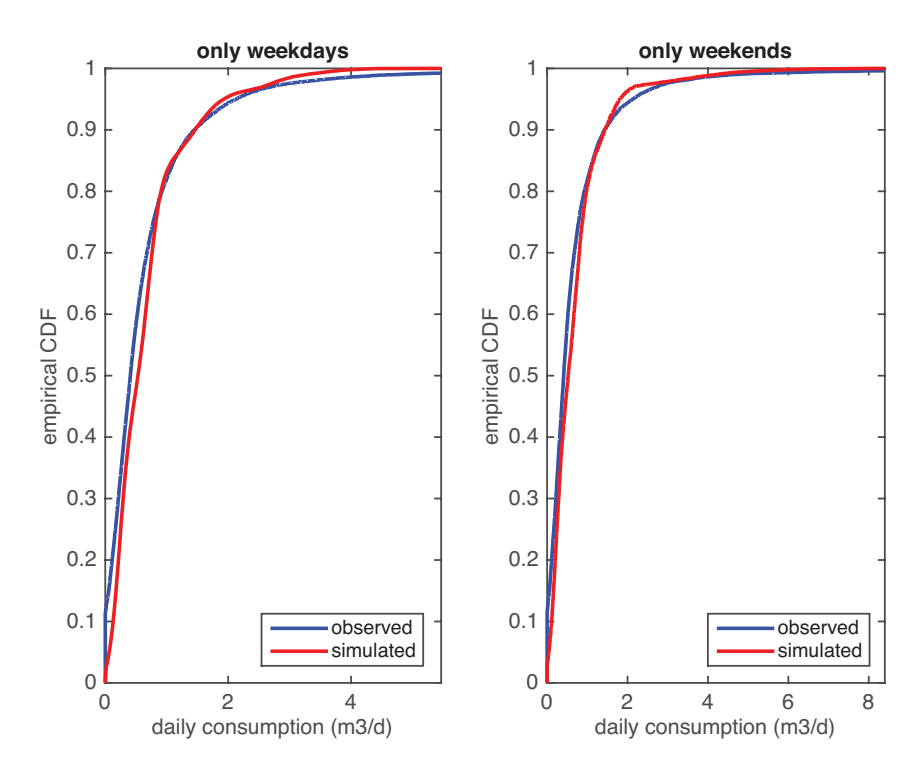


Figure 8: Empirical cumulative density function of daily consumption of SES users, estimated for weekdays (left panel) and weekends (right panel) separately.

Finally, we assessed the quality of our profiles in reproducing the hourly consumption patterns by comparing the empirical CDFs estimated on hourly consumption differentiated depending on different fractions of the days, specifically morning (i.e., from 5 to 9), middle day (i.e., from 10 to 16), evening (i.e., from 17 to 22), and night (i.e., from 23 to 4). The results reported in Figure 9 show that the combination of the daily consumption profiles with the typical load-shapes (Figure 6) allows capturing also the sub-daily variability of water consumption behaviours.

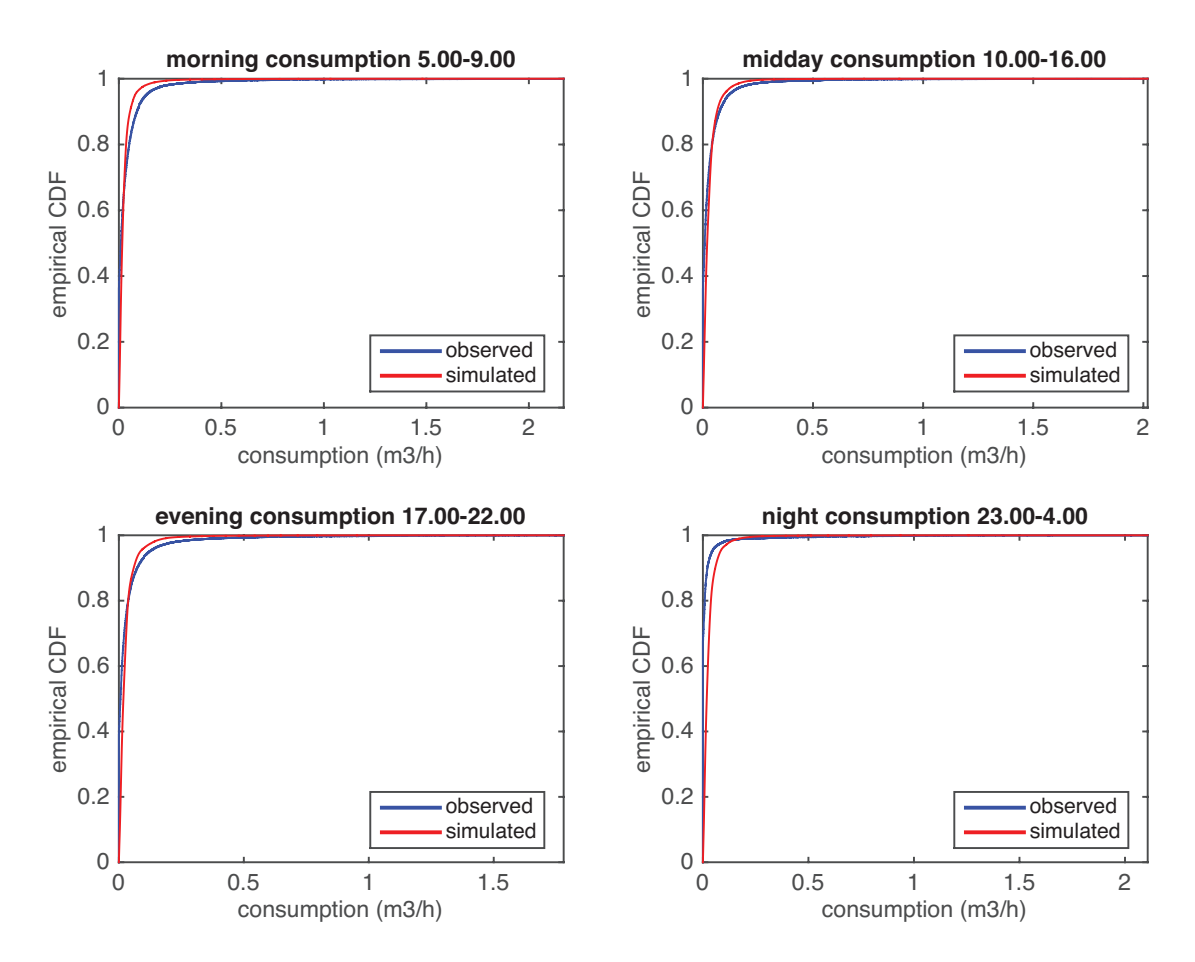


Figure 9: Empirical cumulative density function of hourly consumption of SES users, for different periods of the day.

#### 3.3.2 Spanish case study - EMIVASA

After running the SmartH2O algorithms on the SES dataset, we perform the same experiment on a much larger dataset collected by EMIVASA in Valencia, the second case study of the SmartH2O project. This dataset comprises water consumption readings at 1-hour resolution for a sample of 20,000 users over the time period January 2014 – January 2016. After post-processing, we were able to preserve cleaned data at hourly resolution for over 11,000 users over a time period sufficiently long for running the calibration of the model (over a dataset with an average time series length of 353 days) as well as the validation of the results through the agent-based model (over a two-months period, see Section 4.3.2).

Similarly to the previous case study, since no psychographic variables of the metered users are available (they are being collected through the SmartH2O platform but, currently, these data do not allow a statistically significant representation of EMIVASA customers' population), the construction of the single-user behavioural model is limited to the identification of the consumption profiles, without any multivariate analysis. The simulation of the single-user water consumption is hence obtained by sampling the pdf characterising the identified consumption profiles, following the same hierarchical process applied to data from the Swiss case study (see Section 3.3.1).

In particular, we extracted 4 clusters computed on the average daily consumption and, then, each cluster is partitioned again in two subclasses depending on the day-label (i.e., type of day with typically higher consumption). The resulting profiles, illustrated in Figure 10, show a good

separation of the clusters and also a good distribution of the users among the profiles, with the medium and low profiles containing more users than the high and very high ones. Also, the majority (approximately 66%) of the users show a higher consumption during weekdays, rather than weekends.

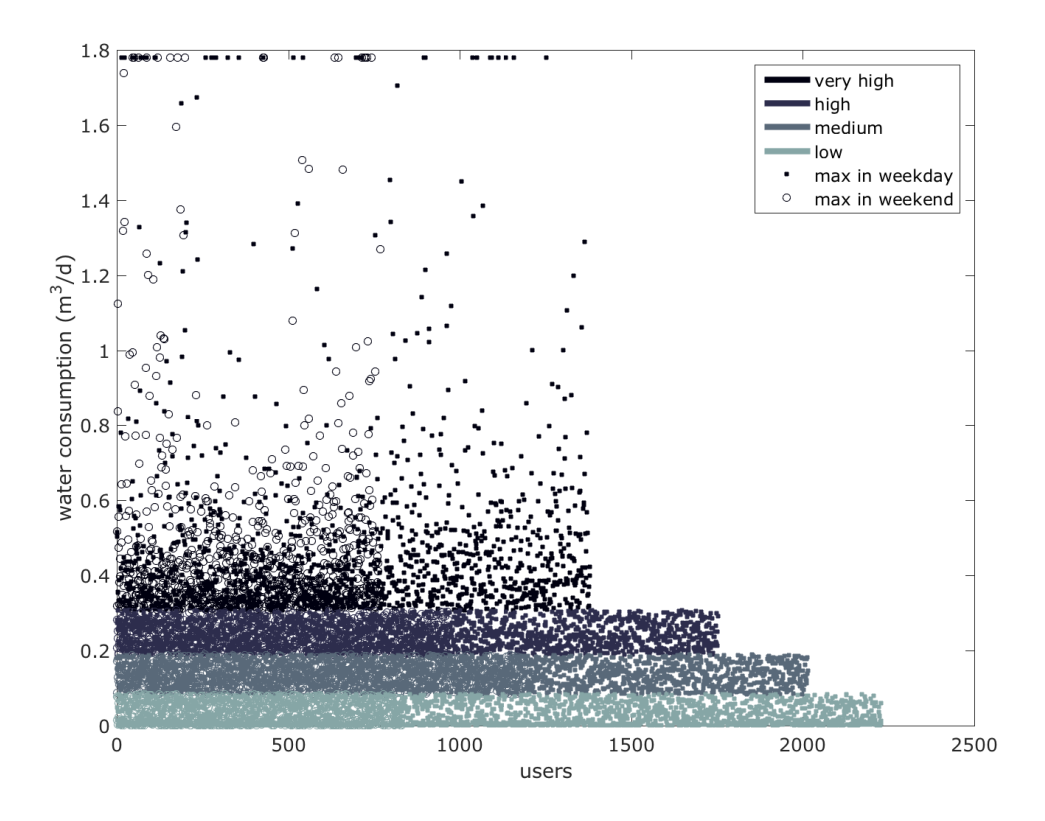


Figure 10. Daily consumption profiles of EMIVASA users.

Each profile is then modelled by estimating two probability density functions (assuming a normal distribution), the first for the daily consumption in weekdays and the second for the daily consumption in weekends. The statistics characterising the 8 probability distribution functions are reported in Table 8. As in the Swiss case study, it is worth noting that the estimated standard deviations are generally slightly larger in weekends than in weekdays, due to more regular routines of the users during the week. Overall, the mean values of consumption found are significantly lower than those of the Swiss case study. On the one hand, we think this is partly due to the dimension of the dataset. Indeed, in the Spanish case study we consider a much higher number of data points and longer monitoring periods, characterized by a large amount of hours with zero consumption, which lower the mean statistics. On the other hand, it is worth noticing that EMIVASA data span over two complete years, while SES data in March-October 2015 are mostly influenced by consumption in the Summer period.

Finally, it is likely that at present the quality of EMIVASA data is higher than that of SES data, simply because smart meters were already installed in Valencia and, therefore, data are not influenced by the warm up period and consequent data anomalies.

Table 8: Statistics associated to the identified consumption profiles. All the values are expressed in m3/d.

Profile	M weekday	Std weekday	M weekend	Std weekend
Very high – max in weekday	0.527	0.287	0.399	0.229
Very high – max in weekend	0.473	0.268	0.523	0.249
High – max in weekday	0.260	0.039	0.198	0.053
High – max in weekend	0.230	0.034	0.267	0.045
Medium – max in weekday	0.149	0.033	0.105	0.041
Medium – max in weekend	0.128	0.030	0.155	0.039
Low – max in weekday	0.035	0.031	0.017	0.022
Low – max in weekend	0.033	0.027	0.048	0.036

From this statistical characterisation of the 8 consumption profiles, we model the single-user consumption behaviours by sampling the corresponding pdfs to generate a trajectory of daily water consumption for each user. Then, the generated trajectory is disaggregated from daily to hourly resolution by using the most typical load-shapes associated to each user. In total, for the Spanish case study we have identified 24 load-shapes, reported in Figure 11. Keeping into account the intrinsic potential variability of load shapes in a pool including several thousand users, we did not further *a posteriori* grouped the 24 load shapes as we did for the Swiss case study. Again, similarly to the previous case study, the most commonly adopted load shapes (top-left of Figure 11) are characterized by a two-peak shape, with the late morning and evening peak. Overall, morning and evening peaks appear delayed, if compared to those obtained from SES data, somehow reflecting the differences in the daily routines for the two case studies. Moreover, in accordance with the previous case study, high-frequency is obtained for the load shape characterizing days/houses with no consumption, ranked second in this case.

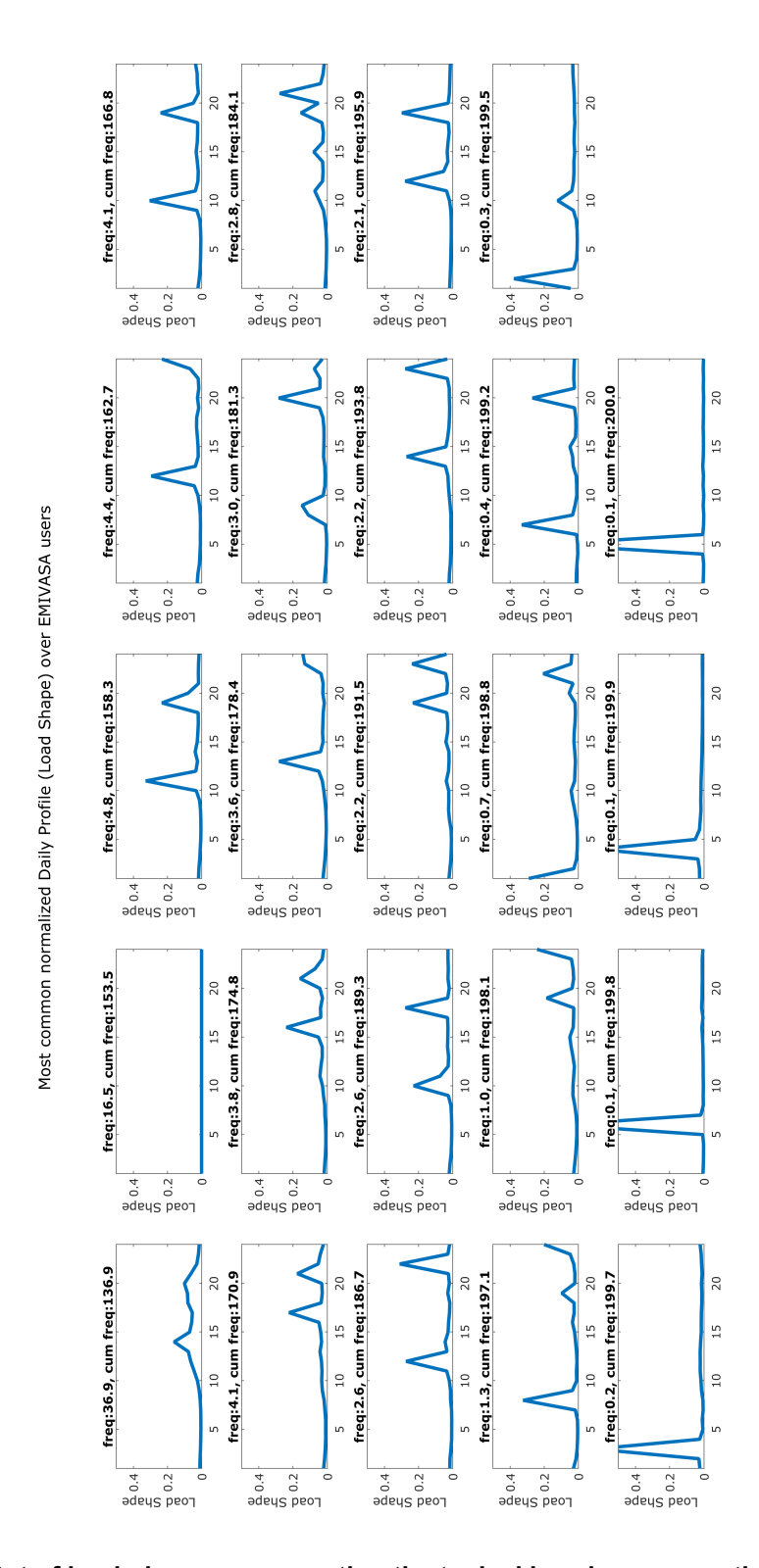


Figure 11. Set of load-shapes representing the typical hourly consumption patterns for EMIVASA users.

We evaluate the accuracy of the modelled single-user behaviours by comparing the simulated consumption over 761 days (i.e. the calibration period Jan 2014 – Jan 2016) against the observed one. Figure 12 shows that the distribution of the simulated daily consumption is very

close to the observed one, with a very small under- and overestimation for medium and high users.

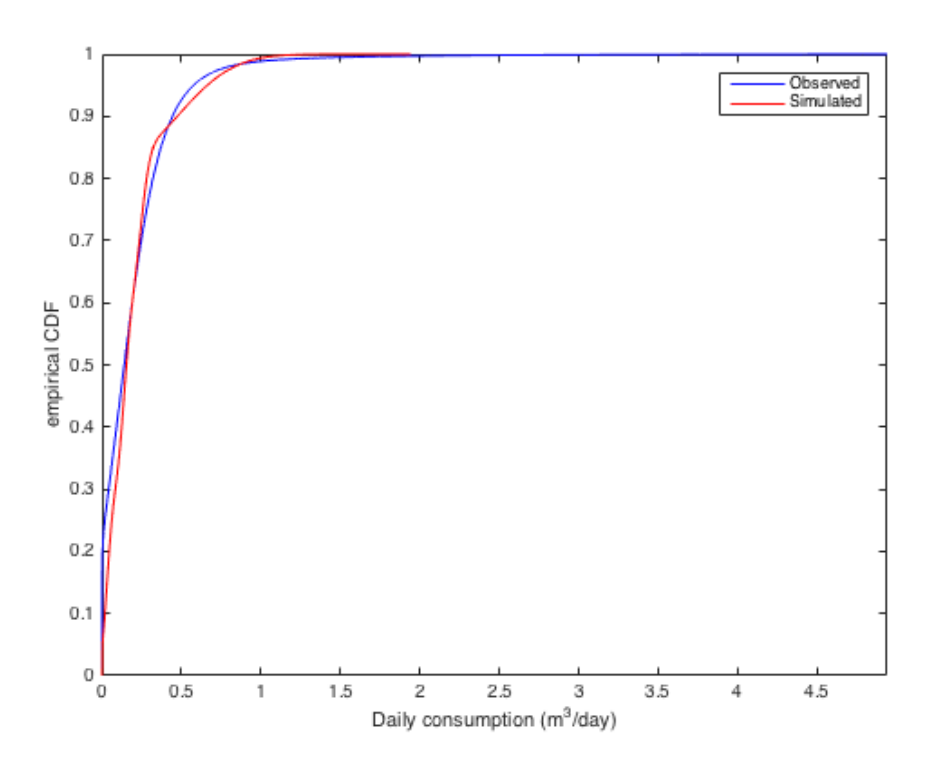


Figure 12. Empirical cumulative density function of daily consumption of EMIVASA users.

A more detailed comparison can be performed by comparing the empirical CDFs of simulated and observed consumption separated for weekdays and weekends, see Figure 13. Results show that our profiles successfully capture the differences in the users' behaviours: despite the consumption during the weekend is generally higher than during weekdays. Both the CDFs computed from simulated consumptions are close to the observed ones. Moreover, the small error in under and over estimating consumption during weekdays explains the small error commented for Figure 12, while the CDF for weekends precisely follows the one of observed data.

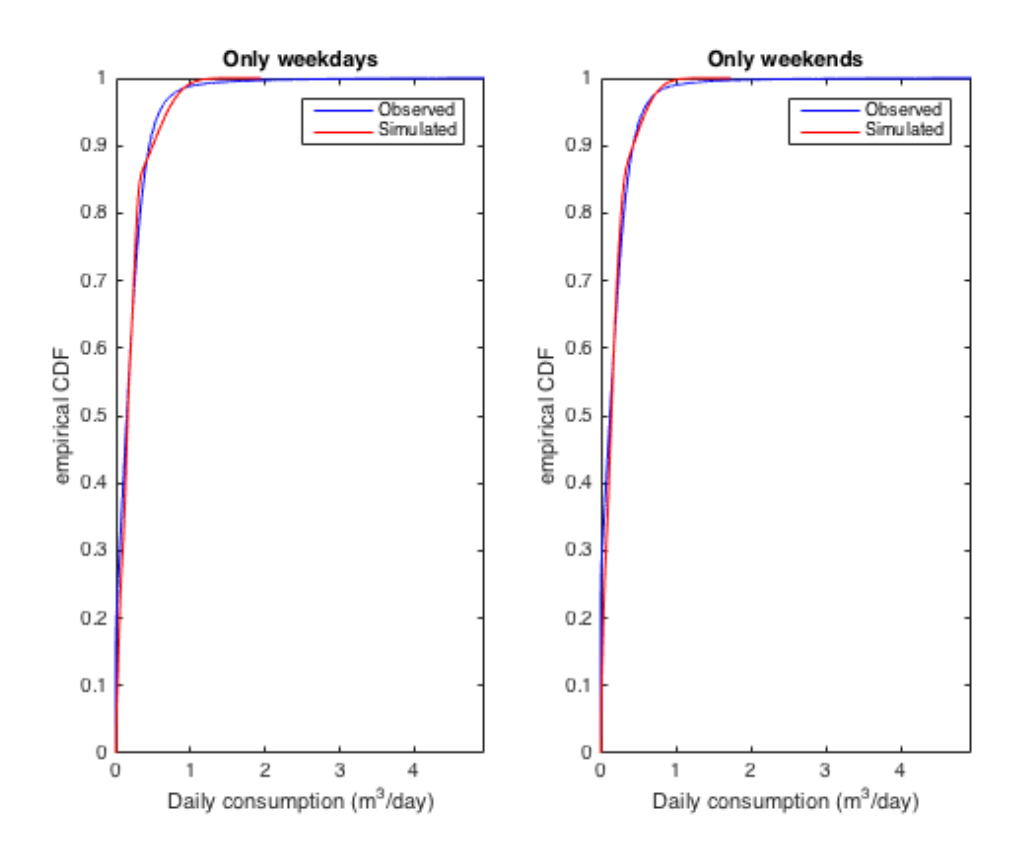


Figure 13. Empirical cumulative density function of daily consumption of EMIVASA users estimated for weekdays (left panel) and weekends (right panel) separately.

Finally, consistently with the analysis performed on SES data, we assessed the quality of our profiles in reproducing the hourly consumption patterns by comparing the empirical CDFs estimated on hourly consumption differentiated depending on different fractions of the days, specifically morning (i.e., from 5 to 9), middle day (i.e., from 10 to 16), evening (i.e., from 17 to 22), and night (i.e., from 23 to 4). The results reported in Figure 14 show that the combination of the daily consumption profiles with the typical load-shapes (Figure 11) allows capturing also the sub-daily variability of water consumption behaviours. In particular, the CDFs of estimated hourly water consumption very precisely follow the distributions of observed data for daily hours after 10 am, when most of water consumption happens. The simulation for night hours is also well performed: in those hours, hourly water consumption is close to zero for almost 90% of the time. Only the CDF of morning consumption (5 to 9 am), is underestimated by our model. As demonstrated by the load-shapes in Figure 11, their morning peak is delayed to day hours later than 10 am. Therefore, the smoothing process embedded in the recursive load-shape extraction algorithm tends to lower down to zero the simulated water consumption in morning hours (before 10 am), as positive hourly consumption in those hours show less frequent occurrences than those after 10am. In order to overcome this model error in future analysis, we will consider keeping a higher number of load shapes that better describe the heterogeneity of early morning consumption, and further sub-dividing day hours in finer intervals for analysis.

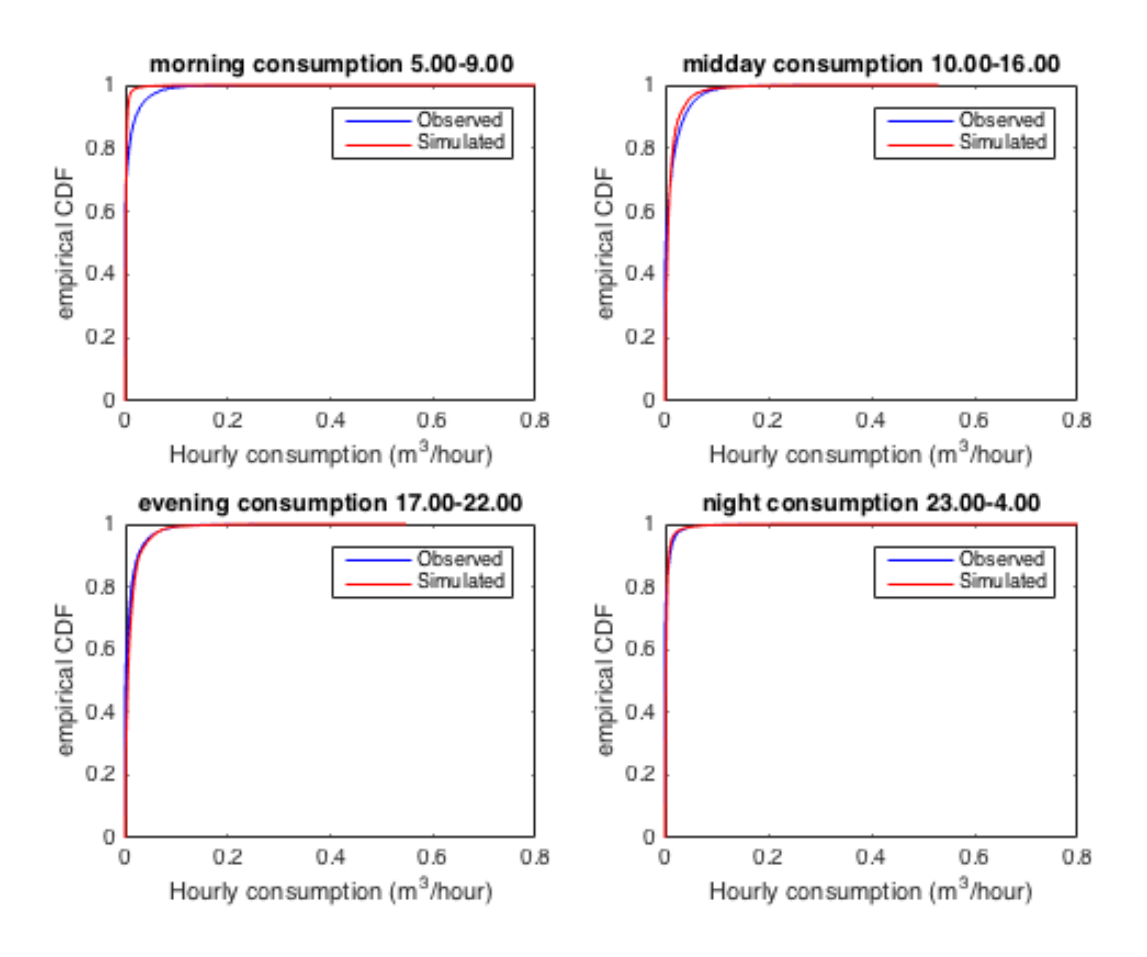


Figure 14. Empirical cumulative density function of hourly consumption of EMIVASA users, for different periods of the day.

#### 3.4 Discussion and recommendation

The results presented in the previous section demonstrates the effectiveness of the SmartH2O algorithms for modelling single-user consumption behaviours. So far, the limitations of the datasets currently available from the SmartH2O test cases, both in terms of time horizon and absence of psychographic data, have constrained the application on SmartH2O data to the identification of consumption profiles.

However, the algorithms presented in Section 3.2 have been demonstrated to be suitable for running both the multivariate analysis as well as the model learning phase. Deliverable D3.2 - First User Behaviour Model reports the application of these algorithms on the *H2ome Smart* project dataset, which comprises more than 3000 households in the towns of the Pilbara and Kimberley Regions of Western Australia. Despite the low resolution of the consumption data, numerical results show the effectiveness of the proposed method in capturing the influence of candidate determinants on residential water consumption profiles and in attaining sufficiently accurate predictions of users' consumption behaviours [Cominola et al., 2015b].

The developed suite of methods is therefore ready-to-use and could be easily integrated in order to perform all the steps of the procedure illustrated in Figure 3 when new data from the SES and EMIVASA users will be available.

## Agent-based modelling

In this section, we describe the developed agent based model for simulating users' consumption behavior accounting for different mechanisms of users' interactions. It updates the model presented in the previous deliverable D3.3 by introducing two diffusion sub-models and a mechanism to capture the effect of price incentives. The application to the two pilots in Terre di Pedemonte (SES utility) and Valencia (EMIVASA utility) are then presented.

After introducing the problem and giving an overview of related works (Section 4.1), in Section 4.2 we describe the general structure of the model as well as its sub-models. In Section 4.3 we then describe the application of the model to SmartH2O data, and assess its capability to model the observed consumption behaviour, the future behaviour under a given pricing policy, and the future behaviour under social norms. Finally, the obtained outcomes are discussed in Section 4.4.

#### 4.1 Problem formulation and related works

In Agent Based Modelling (ABM), agents are defined as autonomous entities that interact with each other and with an environment (see, e.g. [Gilbert, 2008]. ABM constitutes a way to study how low-level and decentralised interactions can influence the ability of a complex system to attain certain objectives.

Because of the aforementioned capability of providing a powerful framework, where to analyse the emergence of macro-structures from individual actions, agent based modelling has become a central tool in addressing the complexity of planning and managing water resources (see, e.g. [Berglund, 2015; Lily et al., 2011], for many references and examples). For an overview of important applications in areas as diverse as physical, biological, social and management sciences see, e.g. [An, 2012; Gilbert, 2008; Balietti et al., 2011].

Two main concurrent views can be isolated depending on the way an agent is encoded in the ABM. The choice mainly depends on the underlying research questions.

According to the first view, agents are *(pro)active*, *goal-directed*, and initiate actions to achieve individual goals. They are thence modelled as utility maximisers [Wooldridge, 2002; Shoham et al., 2009]. According to this approach, it is assumed that the agent's preferences are captured by a utility function, which defines a map from the states of the environment to a real number. Cooperative agents select their actions in order to maximise the total utility at the system-level. A self-interested agent instead chooses a course of action that maximises its own utility. Active ABM "are used to simulate system performance when a set of optimizing actors attempt to achieve individual goal" [Berglund, 2015]. Recent studies developed active ABMs to simulate water users, like farmers or ecological systems, who share water sources [Yang et al. 2009; Giuliani et al., 2013; Giuliani et al., 2015]. Other applications of this approach in water management concerned for instance a group of farmers that select crop and water-use decisions within a shared water basin (e.g. [Barreteau et al., 2000; Becu et al. 2003; Schluter et al., 2007; Ng et al., 2011] or the dynamics of permit holders within the water-pollution trading market [Zhang et al. 2013].

According to the second view, agents are, conversely, *reactive* agents. They are defined as those using a stimulus-response type of behaviour and respond to the present state of the environment [Sycara, 1998]. They do not look at the history or plan their strategy over the future. This characteristic allows the design of simple "if-then" agents behaviours.

Reactive ABM are typically used to simulate the dynamics of a large population of simple actors. As described in great details in the previous WP3 deliverable D3.3, several investigations have used reactive ABMs to understand the complexity of users' behaviour induced by social interaction and thus opinion diffusion mechanisms, but also the influence of meteorological information, water price policies and conservation campaigns. Such applications have focused for instance on the Thames catchment [Barthelemy et al. 2008, Moss et al. 2005], Barcelona [Lopez-Paredes et al, 2005], Valladolid [Galan et al, 2009] and

Thessaloniki [Athanasiadis et al., 2005].

Consistently with our research goal of developing an agent based model for simulating the observed and future water consumption behaviour of a community of users within a district (in this case Terre di Pedemonte and Valencia), we follow the latter reactive agent approach.

## 4.2 SmartH2O agent-based model

This first prototype of the SmartH2O agent-based model presented in Deliverable D3.3 was essentially an input-output model, and thence resembled to the DANUBIA shallow model (Ernst et al. 2005). It predicted future water consumption based solely on the specific values associated to the attributes of an agent, its current level of water consumption and the meteorological sensitivity. Social phenomena and influence mechanisms were not taken into account. The current version, described below, enhances the first prototype by explicitly integrating a social interaction module and a mechanism to capture interaction with water pricing.

The main enhancement in the current model consists in the fact that we have tried to capture the mechanisms underlying the adoption of the SmartH2O portal by water consumers, and its influence on their water consumption. To this aim, we have been inspired by the agent-based model presented in [Galan et al., 2009]. This ABM, a variation of the FIRMABAR agent based model introduced in [Galan et al., 2005], was applied to the metropolitan region of Valladolid. It aimed at simulating and evaluating alternative supply and demand policies under different climatic and technological scenarios, by taking into account the economic, demographic, cultural and spatial processes in the decision making behaviour of households. The tool integrated social sub-models of urban dynamics, water consumption, and technological and opinion diffusion in the ABM, which, in turn, was linked with a geographic information system.

Similarly, we integrate a technological and an opinion diffusion module in our SmartH2O ABM model. The goal of these two modules is to take into account the adoption process of the online portal among users, and the influence of the latter via social pressure on the water consumption.

The overall structure of the model, the two specific modules and their integration within the ABM are discussed below. The SmartH2O model is based on the first prototype described in great details in deliverable D3.3 and is implemented with the commercial simulation software AnyLogic.

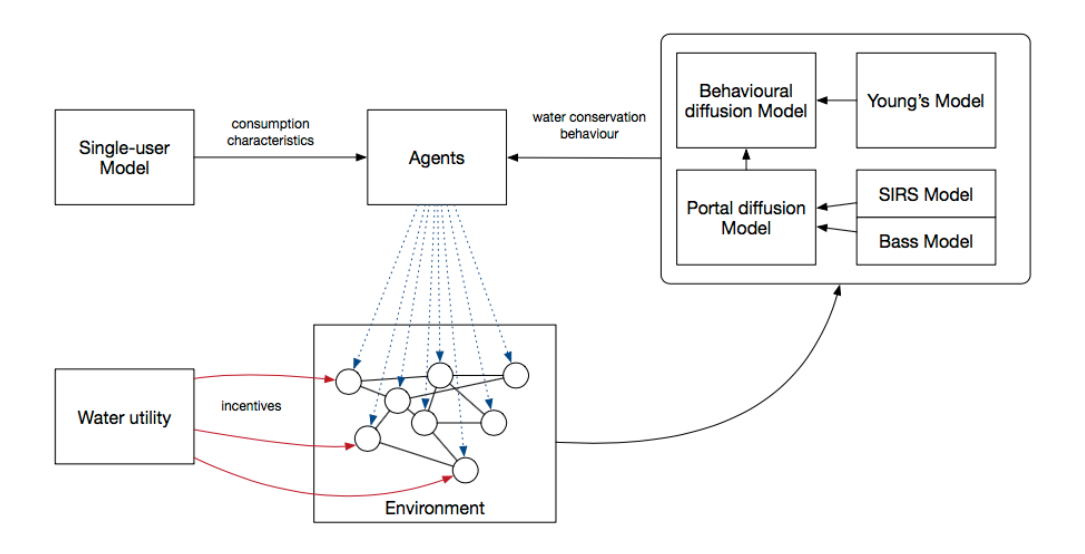


Figure 15: General SmartH2O agent-based model structure.

#### 4.2.1 General SmartH2O agent-based model structure

The model consists of different sub-modules aimed at capturing various influential aspects of water demand in urban area. To understand them, we first explain the general structure of the model

The underlying general structure is essentially the same as the one of the first prototype. In addition to the *Main* agent acting as the environment for all other agents, the ABM includes two main agent's types:

- the Supplier type;
- the Household type;

and other types instrumental to the behaviour of the model (for instance the *Consumption Request* agent type, or the *Consumption Type* agent and its extensions).

The role of the *Supplier* agent is to be responsible for asking the households about their daily consumption, and thus initiating the interaction phase at each simulation step, informing the households agents about any change in the price policy, and enhancing campaigns for the adoption of the on-line portal.

Household agents are generated when the model is initialised. Contrary to their location in the environment, attributes of households are not generated randomly. They correspond to the ones introduced and discussed in the WP3 deliverables D3.1 and D3.2. The consumption characteristics of each household come from the single-user model. Together with the consumption function, they are described in details Section 4.3.1.

Since agents are reactive, they are encoded with a set of behavioural rules that respond to signals from the environment and that play a role in the diffusion models introduced below and more extensively described in the next sections. Several variables can affect users' water consumption. A key factor is the role of technology and, in our specific context, the role of the SmartH2O portal. To incorporate its role and thence assess its influence, we have defined two sub-models. Firstly, since the adoption and diffusion of technology, i.e. the portal in our case, is not an immediate process, but depends on the interaction among users, as well as on adoption campaigns initiated by authorities, we have incorporated a technology diffusion model. Secondly, we want to take into account the role of the SmartH2O portal with respect to the social attitude of the population towards the water resource. To this aim we use a behavioural diffusion model to capture the spread of social awareness and thus of a sustainable water consumption behaviour thorough the usage of the SmartH2O portal. Another direct key factor is seasonality. To capture this factor, an estimation of the seasonality parameters discussed in [Griffin et al., 1991, Chang et al. 2014] has been integrated homogeneously into the water consumption function of households as a monthly multiplicative factor. Lastly, price can act as an incentive towards users' water conservation behaviour (see deliverable D.5.1 for an extensive review of pricing instruments). Based on the results of the pricing survey (conducted in Ticino among SES customers) from WP5, to be presented in D.5.4, we have also incorporated a mechanism to capture the impact on consumption of a price policy. This is explained in Section 4.3.3.

#### 4.2.2 Portal diffusion model

Empirical data suggests that the diffusion of a technological innovation, in terms of the cumulative number of adopters, very often conforms to an S-shaped curve. Such curves are characterised by a slow initial growth, followed by a rapid growth and finally by slow growth toward a definite upper limit [Maede et al., 2006]. A well-known, successful and simple model that explains such behaviour has been proposed by [Bass, 1969]. By considering the dynamics of the population, Bass suggests that individuals are influenced by a desire to innovate (coefficient of innovation c) and by a need to imitate others who already have adopted the

concerned technology (coefficient of imitation s). The adoption rate at time t, is thence driven by

$$c + s \cdot \frac{N(t)}{m}$$

where N(t) is the accumulated number of adopters, and m is the size of population.

The Bass model, and in general diffusion models, can be seen as models of the spreading of an epidemic. From this perspective, imitation is thence seen as a contagion phenomenon. It is therefore natural to consider other models of infectious diseases to characterise the diffusion of innovation (see, for instance, [Capasso, 2008]), for an in-depth overview of epidemic models).

When dealing with a large population, deterministic epidemic models are used. In a deterministic model, the population is partitioned in a certain number of subgroups, each determining the stage of the epidemic. The most used subgroups are:

- Susceptibles (denoted with the letter S), i.e. individuals who have not been infected but are at risk.
- Infective (I) individuals, who are infected and are capable of transmitting the disease.
- Recovered (R) individuals, who, for some reason, can no longer contract the disease.

The SIR model [Kermac et al., 1927] is probably the most basic epidemiology model. It assumes that the population is well mixed, and that it is closed (no births or deaths, no migration). It is thence defined by the following differential equations:

$$\frac{dS}{dt} = -\frac{bSI}{I}$$

$$\frac{dI}{dt} = \frac{bSI}{I} - gI$$

$$\frac{dR}{dt} = gI$$

where: *b* is the contact rate and *g* is the recovering rate.

A natural relaxation of the model is to allow members of the recovered class to be free from the infection and to join anew the susceptible class. The so called SIRS model [Kermac et al., 1933] is therefore the model obtained from the SIR model by:

$$\frac{dS}{dt} = -\frac{bSI}{I} + fR$$
$$\frac{dI}{dt} = \frac{bSI}{I} - gI$$
$$\frac{dR}{dt} = gI - fR$$

where the new parameter *f* is the free of infection rate.

Our portal diffusion model is thence a Bass model coupled with features of an epidemic SIRS to capture the fact that adopters can decide to stop using the adopted technology (for a while), in our case the SmartH2O portal. The dynamic stock and flow diagram corresponding to the portal diffusion model is presented in Figure 16 below.

We followed the methodological approach described in [Borshchev et al., 2004] to implement differential equations into the agent based model.

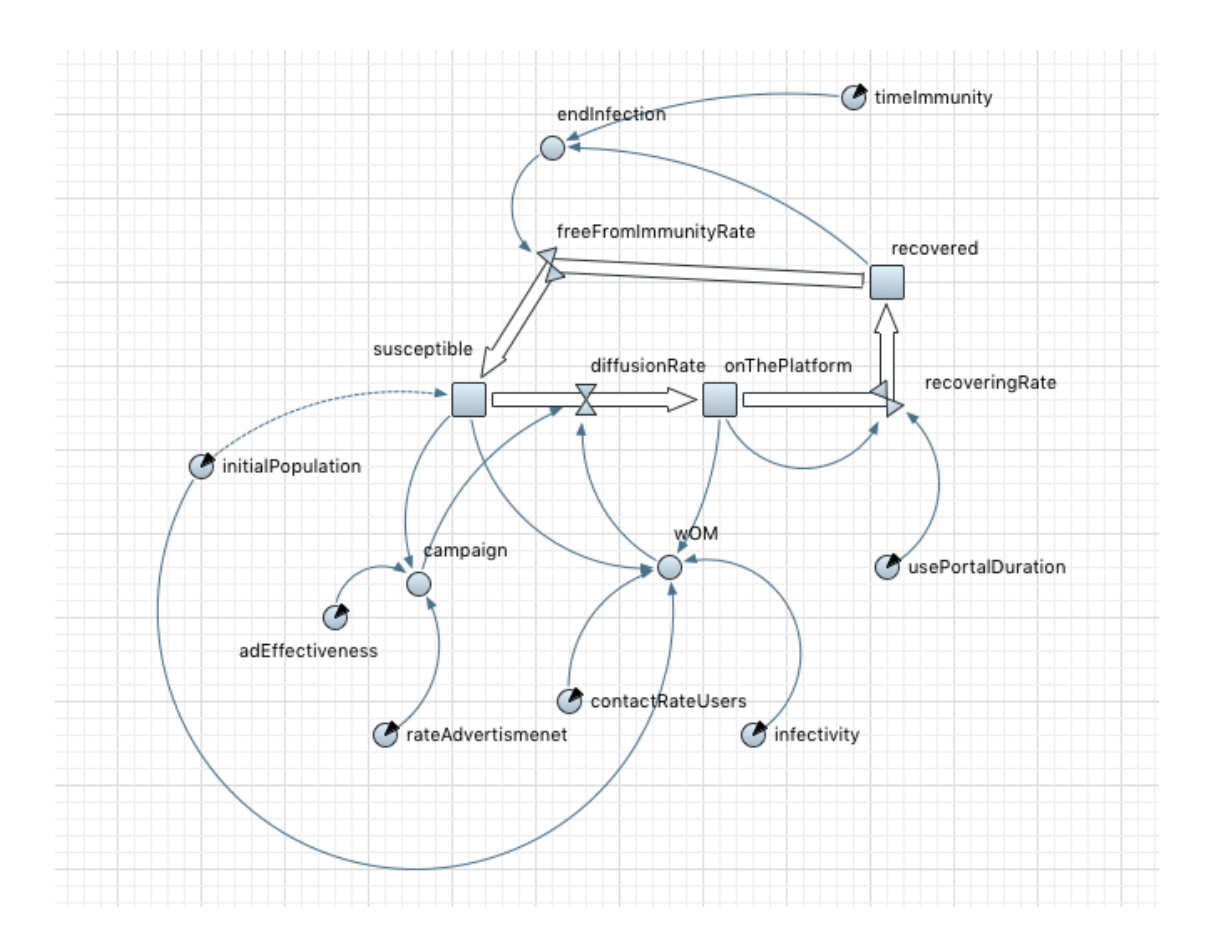


Figure 16: Stock and flow diagram of the SmartH2O portal diffusion model.

#### 4.2.3 Behavioural diffusion model

The adoption of social norms often follows a pattern similar to the spread of an epidemic too. In many cases, it is indeed the result of a diffusion process through a social network, characterised by the fact that a certain behaviour is influenced by the number of contacts (neighbours) that have adopted such same attitude, hence giving rise to positive reinforcement. This is the view behind the structure of the additional behavioural module we have introduced in the SmartH2O ABM. As depicted in Figure 16, the behavioural diffusion model is implemented as a plug-in of the portal diffusion model. The aim of this module is to capture the role of the SmartH2O portal with respect to the social attitude of the population towards a sustainable water consumption behaviour. The adopted model is the so called Young diffusion model [Young, 2003; Young, 2011]. It is a reversible stochastic diffusion model that has been successfully employed in the study of the domestic water management in Valladolid metropolitan area [Galan et al., 2009] and of the Orb river in [Edwards et al. 2005]. The model assumes that a household, while it is a portal adopter, can choose over time between a behaviour E (environmentalist) and a behaviour NE (non environmentalist). The model considers a decrease in water consumption as consequence of E behaviour. In turn, the choice of a behaviour is determined by a utility function U that depends on:

- The agent's current behaviour;
- The behaviour of its social network;

- An exogenous parameter (*p*) that measures the social pressure towards behaviour E. The graph structure of the network among portal users is always assumed to be a clique. The utility function of household A for adopting behaviour E or behaviour NE are defined by the following expressions:

$$U(A, E \to E) := a.V(A, E) + p;$$
  

$$U(A, \neg E \to E) := a'.V(A, E) + p;$$
  

$$U(A, E \to \neg E) := b.V(A, \neg E);$$
  

$$U(A, \neg E \to \neg E) := b'.V(A, \neg E);$$

where the formula  $U(A, x \to y)$  determines the utility for A to change behaviour x into behaviour y; a, a, b, b' are parameters measuring the weight (importance) given to neighbours' behaviour, and V(A, x) is the proportion of households in A's network that have adopted behaviour x.

To take into account the variability of the response when an agent updates its behaviour, the probability of choosing a given action is assumed to be a logistic function of the payoff difference between the two actions, in the Young model. More precisely, the probability of choosing behaviour E for agent A, when E is its current choice, is given by the Young's formula:

$$\Pr(A, E \to E) \coloneqq \frac{e^{\left(U(A, E \to E) - U(E, E \to \neg E)\right)}}{1 + e^{\left(U(A, E \to E) - U(A, E \to \neg E)\right)}}$$

The probability of choosing NE is, of course, one minus this quantity. Analogous formulas define the dual cases. This probabilistic update function is initialised at each time step, when the household receives the message from the supplier asking it to calculate the water consumption.

In our framework households are created with or without a predisposition for adopting behaviour E once on the portal (the percentage among the population of households born with a predisposition being not null). When an agent with such a predisposition becomes a portal adopter, it will instantaneously behave according to E. In the case it does not have such a predisposition, it will on the contrary start acting according to behaviour NE. As mentioned in the description of the general structure of the model, at beginning of each round, each household receive a message from the Supplier asking to calculate its water consumption. Before such a calculation, a household updates its behaviour according to the appropriate Young's formula, provided it is a portal user. In case of behaviour E (and if the agent is on the platform), a lowering factor is thence applied to the result of the consumption calculation.

## 4.3 Application on SmartH2O data

In this section, we apply the agent-based model to the two pilot case studies of Terre di Pedemonte and Valencia. While waiting for data coming from the two platforms concerning the social networks of contacts of users, we have hypothesised and tested two different networks: firstly, a distance based network, and then a scale free network.

#### 4.3.1 Modelling observed behavior: Swiss case study - SES

The single-user behavioural model described in Section 3 was run on the dataset collected by SES during the SmartH2O project over the time period March 2015 – October 2015. The used dataset comprises water consumption readings at 1-hour resolution for 256 users. During the initialisation process of the SmartH2O ABM, a household agent is generated for each user.

Since no psychographic variables of the metered users are available (they are being collected through the SmartH2O platform, but the small size of the sample data collected so far does not allow for a statistically significant representation of SES customers' population), the only attribute of a household agent is the Smart meter ID.

Based on the outputs generated by the single-user model, a consumption class C, a consumption profile class for the week-end P(1), and a consumption profile class for the week-days P(2) are associated to each household H. This triple (C, P(1), P(2)) constitutes the consumption profile of agent H.

The procedure for calculating the consumption is the following:

- Firstly, agent H verifies the type of day for the current day, i.e. week-day (2) or weekend (1). Based on this information (let's call the type of day D) and on its consumption class C, it determines the 10 bins and the associated probability distribution. It thence chooses accordingly a bin, and uniformly samples a value within the bin range. This value (X), multiplied by the seasonality factor, constitutes its daily water consumption.
- Secondly, the agent has to determine the hourly distribution of its consumption, i.e., for each hour h, the percentage of X that it will consume during hour h of the current day. To do so, it considers the pair (D, P(D)) and determines the list of possible load profiles and the corresponding probability distribution accordingly. It thence randomly extracts a profile according to such distribution. The chosen profile will provide for each hour of the day the amount of consumed water during that hour.

The performance of the model without the diffusion sub-modules has been evaluated by considering a period ranging from 1/11/2015 to 31/1/2016 against the observed SmartH2O for the same period. The tested model can therefore be seen as an input-output model based on the implementation of the single user model coupled with a mechanism capturing the influence of meteorological characteristics on water consumption. The corresponding seasonality multiplicative factors are 0.75 for November, 0.725 for December and 0.7 for January. For each month we have computed the average aggregate daily water consumption. Table 9 summarises the obtained results based on 25 simulations (average values are reported in the first column, standard deviation in the second column) and compare them to the average daily consumption obtained from the data coming from the SmartH2O database of the district of Terre di Pedemonte (third column). It shows that the consumption forecasts provided by the model are quite close to the real water usage.

Table 9: Forecasting consumption results of Terre di Pedemonte's users.

	Mean [m³/day]	Standard deviation	Average user daily consumption in Terre di Pedemonte [m³/day]
November	0.508	0.002	0.469
December	0.489	0.002	0.448
January	0.473	0.002	0.427

The gap estimation is of 8.3% for November, 9.1% for December, and 10.7% for January. Such gaps are motivated by the fact that the single-user model, on which this input-output version of the ABM is based, was run on data coming from on a very limited period (6 months: from March 2015 to October 2015), thus not including the winter period: this led to a slight overestimation of the daily average consumption of single households.

#### 4.3.2 Modelling observed behavior: Spanish case study - EMIVASA

The single-user behavioural model was run on a dataset collected by EMIVASA over the time period January 2014 – January 2016. After post-processing, the used dataset comprises water consumption readings at 1-hour resolution for over 11,000 users. As for the Swiss case study, during the initialisation process of the SmartH2O ABM, a household agent is generated for each user.

The performance of the model without the diffusion sub-modules has then been validated against the observed data in Valencia during the period 2/1/2016-1/3/2016. The corresponding seasonality multiplicative factors are 0.7 for January and 0.725 for February. As for the previous case study of Terre di Pedemonte, for each month we have computed the average aggregate daily water consumption. Table 10 summarises the obtained results based on 10 simulations (average values are reported in the first column, standard deviation in the second column) and compares them to the average daily consumption obtained from the data coming from the EMIVASA database of Valencia (third column). It shows that the consumption forecasts provided by the model are very close to the real water usage.

Table 10: Forecasting consumption results for Valencia.

	Mean [m³/day]	Standard deviation	Average user daily consumption in Valencia [m³/day]
January	0.222	0.016	0.221
February	0.231	0.016	0.227

The gap estimation is of 0.45% for January and 1.7% for February. The performance could be even tighter, once the available observed data will cover a longer period and better suited seasonality factors can be estimated from them.

#### 4.3.3 Modelling future behaviour under pricing policies

In this section, we model, in cooperation with WP5, a scenario in which a price shock is applied. More precisely, we consider the case in which there is an increase in the semester bill of 40 CHF. To model such scenario, we rely on the results of the pricing survey (conducted in Ticino among SES customers). The full results of the survey will be discussed in D5.4. Such results were used to assess different types of incentive responses. In the survey, two incentive measures were tested (environmental badge vs. bill increase). Respondents were asked whether they would alter specific consumption habits under the conditions described in the scenario. In this section of the deliverable we focus on the bill increase incentive measure. First of all, from the preferences expressed in the survey, it turns out that users can be classified in 5 different classes depending on the duration of their shower. Then, for each class we observed the response in term of a possible reduction in the duration of a shower determined by a price increase of 40 CHF, corresponding to an increase between 23% and 43% of the reference bill range. The results of the survey are reported in Table 11 below.

From Table 10, we notice that users from class A are ready to reduce their showertime of ca 26%, users from class B of ca 11%, users of class C of ca 8%, users of class D of ca 7%, and users of class E of ca 6%.

Table 11: Response of users to a 40 [CHF/ (semester per household)] price increase.

Class		Showertime	Showertime reduction		
Name	Frequence	[min]	Mean [min]	St. deviation	95% c.i.
Α	46.93%	1-5	0.65	0.15	0.36 - 0.94
В	45.33%	5.1-10	0.85	0.14	0.58 – 1.12
С	6.40%	10.1-15	1.03	0.19	0.64 – 1.42
D	1.07%	15.1-20	1.22	0.28	0.67 – 1.77
Е	0.27%	20.1-22	1.33	0.33	0.68 – 1.98

In the absence of data about showertime and the associated water consumption volumes from SES users in Terre di Pedemonte or EMIVASA users in Valencia, we follow the statistics from *The American Water Works Association Research Foundation*, "Residential End Uses of Water", 1999, according to which 16% of residential water consumption is due to showering. We therefore implement in the SmartH2O ABM the following mechanism. When a household agent is created, a showertime class among A, B, C, D, E is associated according to the associated probabilities. Thence, an if-then rule stating that whenever a 40 [CHF/(semester per household)] price increase is performed (this is performed only once), then an agent applies the result of the probabilistic function coded in Figure 11 as a multiplicative factor into the water consumption function, determining the lowering percentage in water consumption due to shower time reduction as response to a price shock. Such reduction depends on the showertime class associated to an agent.

In Figure 17, APE is the normal distribution function corresponding to the showertime results from the WP5 survey, while SR is the normal distribution function of the showertime reduction results from the WP5 survey. The characteristics of such functions depend on the showertime class, and are defined according to Table 11.

In the aim of assessing the price increase rule, we have performed 25 simulations in which the price shock policy is performed at the beginning of the year 2016. Notice that also in this case the model does not include the diffusion sub-modules. We have thence considered as output the daily average water consumption for the month of January 2016. The results are reported in Table 12, where they compared to the results from the simulations for the same month described in Section 4.3.1.

Table 12: Price increase scenario results.

	Mean	[m³/day]	Standard deviation	Reduction consumption
January	0.461		0.002	2.54%

```
//check showertime class A
if (ShowerReductionPerc <= 46.93)
{
//Average price effect
double APE = normal(0.3581828, 0.9354394, 0.6468111, 0.1466796);
//Showertime reduction
double SR = uniform(1,5);
double ret= (0.16*(APE / SR));
//check showertime class B
else if (ShowerReductionPerc <= 92.27)
//Average price effect
double APE = normal(0.5784367, 1.12123, 0.8498334, 0.1379226);
//Showertime reduction
double SR = uniform(5.00001,10);
double ret= (0.16*(APE / SR));
//check showertime class C
else if (ShowerReductionPerc <= 98.67)
//Average price effect
double APE = normal(0.6511131, 1.417685, 1.034399, 0.1947842);
//Showertime reduction
double SR = uniform(10.00001,15);
double ret= (0.16*(APE / SR));
//check showertime class D
else if (ShowerReductionPerc <= 99.73)
//Average price effect
double APE = normal(0.6728157, 1.765114, 1.218965, 0.2775506);
//Showertime reduction
double SR = uniform(15.00001,20);
double ret= (0.16*(APE / SR));
//check showertime class E
else
//Average price effect
double APE = normal(0.6765592, 1.982849, 1.329704, 0.3319254);
//Showertime reduction
double SR = uniform(20.00001,22);
double ret= (0.16*(APE / SR));
return ret;
```

Figure 17: Body of the function calculating the lowering factor due to showertime reduction; 'normal' is the AnyLogic (truncated) normal distribution function.

From the results presented in Table 12, we see that there is a 2.54% reduction with respect to the aggregate consumption in a scenario where no price policy is adopted. The results summarised in Table 12 are consistent with the fact that, if we calculate the expected reduction by considering the result from the survey presented in Table 11, we obtain the following rough estimation:

```
16\% \times (46.93\% \times 26\% + 45.33\% \times 11\% + 6.40\% \times 8\% + 1.07\% \times 7\% + 0.27\% \times 6\%) = 2.84\%.
```

The results of the simulations show therefore that the if-then rule introduced in the model allows capturing the expected reduction in water consumption due to showertime reduction as reaction to a bill increase of 40 [CHF/(semester per household)].

#### 4.3.4 Sensitivity analysis of the portal diffusion model

We designed a 2<sup>4</sup> factorial experiment to verify the influence of the different sets of parameters (factors) on the behaviour of the portal diffusion model. The chosen factors are:

- A: the advertisement campaign, given by parameters adEffectiveness and rateAdvertisment;
- B: the word of mouth, given by parameters *contactRateUsers* and *infectivity*;
- C: the duration of the use of the portal, given by parameter usePortalDuration;
- D: the duration of the immunity time, given by parameter timeImmunity.

We are interested in two levels for each factor: high (+) and low (-). The description of the levels for factors A, B, C, and D is reported in Table 13.

Table 13: Coding chart for the factors in the portal diffusion model.

Factor	Parameter	+	-
Α	adEffectiveness	90%	1%
	rateAdvertisement	1/day	1/month
В	contactRateUsers	1/day	1/month
	infectivity	90%	1%
С	usePortalDuration	3 months	1 week
D	timeImmunity	3 months	1 week

We set the initial population of experiment design at 256 users, similarly to the size of SES customers community that we are metering at hourly resolution. The behaviour of the system is similar in each experiment: the number of users grows relatively quickly following a S-shape behaviour until the maximum is reached. Then (usually) it collapses towards the equilibrium as depicted in Figure 18.

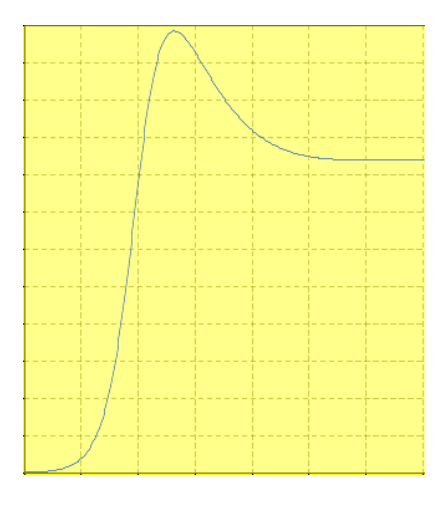


Figure 18: Dynamics of the number of portal users in the portal diffusion model.

The responses of the experiments are therefore:

1. the percentage of users on the portal at equilibrium point of the system;

2. the maximal percentage of users on the portal reached by the system.

The results are summarised in Table 14. In Table 15, we describe the main effect for each factor on the responses, while in Table 16 we describe the interaction effect for each pair of factors on the responses.

Table 14: design matrix of the 2<sup>4</sup> factorial experiment for the portal diffusion model.

Factor	Factor A	Factor B	Factor C	Factor D	Respons	ses
combination					Eq.	Max
1	+	+	+	+	49.8%	96.7%
2	+	+	+	-	92%	97%
3	+	+	-	+	7.1%	78.1%
4	+	+	-	-	47.4%	78.7%
5	+	-	+	+	49.7%	94.7%
6	+	-	+	-	91.7%	95.4%
7	+	-	-	+	7.1%	70.7%
8	+	-	-	-	46.3%	71.6%
9	-	+	+	+	49.4%	93.5%
10	-	+	+	-	91.6%	94.7%
11	-	+	-	+	6.1%	55.3%
12	-	+	-	-	42.1%	59.2%
13	-	-	+	+	2.9%	2.9%
14	-	-	+	-	3%	3%
15	-	-	-	+	0.2%	0.2%
16	-	-	-	-	0.2%	0.2%

As expected, from Table 15 we observe that all three factors have an effect on equilibrium (just remember that the sign minus in the fifth row means that increasing the duration of immunity means lowering the number of platform users). On the other hand, for what concerns the maximum reached by the system, we notice that, contrary to the other factors, the value of the immunity time does not show any significant effect. This is also consistent with what we expected from the structure of the model.

Table 15: Effect on responses for each factor.

Factor	Effect on equilibrium	Effect on maximum
Α	24.45%	46.74%
В	17.81%	31.94%
С	34.20%	20.49%
D	-30.25%	-0.96%

Table 16: Effect of interaction on responses.

Factors	Effect of interaction on equilibrium	Effect of interaction on maximum
AB	-22.675%	-34.79%
AC	9.62%	0.69%
AD	-10.34%	-0.57%
ВС	10.82%	7.1%
BD	-9.92%	-0.53%
CD	-1.37%	0.39%

Results reported in Table 16 show that the highest effect on the responses of the system under investigation emerges from the interaction between factors A and B. As the sign is negative, this means that the effect becomes noticeable when levels are opposite. This can be understood in light of the fact that if one of the two factors is low, keeping the other high enables to keep the responses high, while coordinating the level of both factors does not have a significant incidence on the response of the system. For what concerns the equilibrium, we can also see that coordinating the levels of either factor A or B with the level of C has an impact on the behaviour of the system. The dual phenomenon clearly happens when factor D is considered instead of C. This was to be expected in virtue of the structure of the model. Finally, we remark that the interaction between factors C and D is negligible.

#### 4.3.5 Modelling future behaviour under social norms: Swiss case study - SES

One of the aspects we want to capture thorough the ABM is the emergence of social norms related to water consumption among a population of users. To this aim we introduced the two diffusion sub-models described in Section 4.2 and applied them to the Terre di Pedemonte case study. Given the exploratory nature of the work due to the absence of data on which to calibrate the behaviour diffusion model, we have parameterised it by looking at analogous models applied to other European municipalities. The Young's model has been parameterised following the work by [Edwards et al., 2005] on the Orb river (Herault, France), and by [Galan et al., 2009] in their study of Valladolid metropolitan are. These values are a=b'=0.7, and a'=b=0.3, see Section 4.2.3. Another important parameter related to the Young's model is the percentage of households characterised by a predisposition for behaviour E. For determining such value, we rely on the results of the survey conducted in WP5 on SES users described in the previous section. In this section of the deliverable we focus on the badge increase incentive measure of the survey. Based on the study, WP5 was able to estimate a model in which:

- 1. The answer of the users is positive if they engage themselves to reduce the water consumption at the same time each of the following actions: showering, gardening, watering plants (both indoor and outdoor), using the washing machine;
- 2. The chosen observations concern the subclass of users able to perform all the aforementioned actions.

We thus notice that symbolic incentives increase of 10.8% the probability of a user to reduce its daily water consumption. Based on this observation, we thence assume that with a probability of 10.8% a user born with a predisposition of reducing its water consumption once on the portal. See that, from the point of view of social norm, a reduction on the aggregate water consumption depends solely on the number of users adopting behaviour E, we have

analysed the impact of the external information p in the Young's sub-model. Such parameter could be interpreted as measuring the social pressure towards a behaviour respectful of the environment, or more specifically the success of civic education or efficiency programs as policy instruments to reduce water demand. Notice that the behaviour of the Young's model does not affect in this formulation of the ABM the behaviour of the portal diffusion model.

The robustness of the ABM model to the parameter p has been assessed for 4 different scenarios. Such scenarios are generated based on the analysis on the portal diffusion model performed in Section 4.2.2. Their characteristics are depicted in Table 17.

Table 17: Description of the scenarios for the Terre di Pedemonte case study.

Scenario	Factor A	Factor B	Factor C	Factor D
	rateAdv.   adEffect.	contactRate.   infect.	usePortalD.	timeImmunity
1	1/week   10%	1/week   10%	3 months	3 weeks
2	1/week   10%	1/week   10%	1 month	3 weeks
3	1/month   5%	1/month   5%	3 months	3 weeks
4	1/month   5%	1/month   5%	1 month	3 weeks

We therefore have that, in all scenarios,

- we keep factor D at the same (medium) level: 3 weeks;
- we coordinate the levels of factors A and B.

In all scenarios, we are interested in keeping track of

- the aggregate water consumption's level;
- the number of users of the portal;
- the number of users of the portal that have chosen behaviour E.

According to the results of the efficiency of the usage of the WaterSmart software (<a href="http://www.watersmart.com/measurable-results/">http://www.watersmart.com/measurable-results/</a>) we assume that choosing behaviour E implies a reduction of 5% in water consumption. For each scenario, we perform a sensitivity analysis with respect to parameter p in the Young model (see Section 4.2.3). We thence consider 5 sub-scenarios depending on the value of p. We assume that this value ranges over  $\{0, 0.25, 0.5, 0.75, 1\}$ . For each sub-scenario, we perform 10 runs of one year (from January 1st until end December), and consider as output (a) the number of portal users who have chosen behaviour is E, and (b) the aggregate water consumption. The results concerning the number of users who are on the portal and whose preferred behaviour is E is given in Figure 18 below. Before, in Figure 17 we report the results on the fraction of users who are adopting the portal.

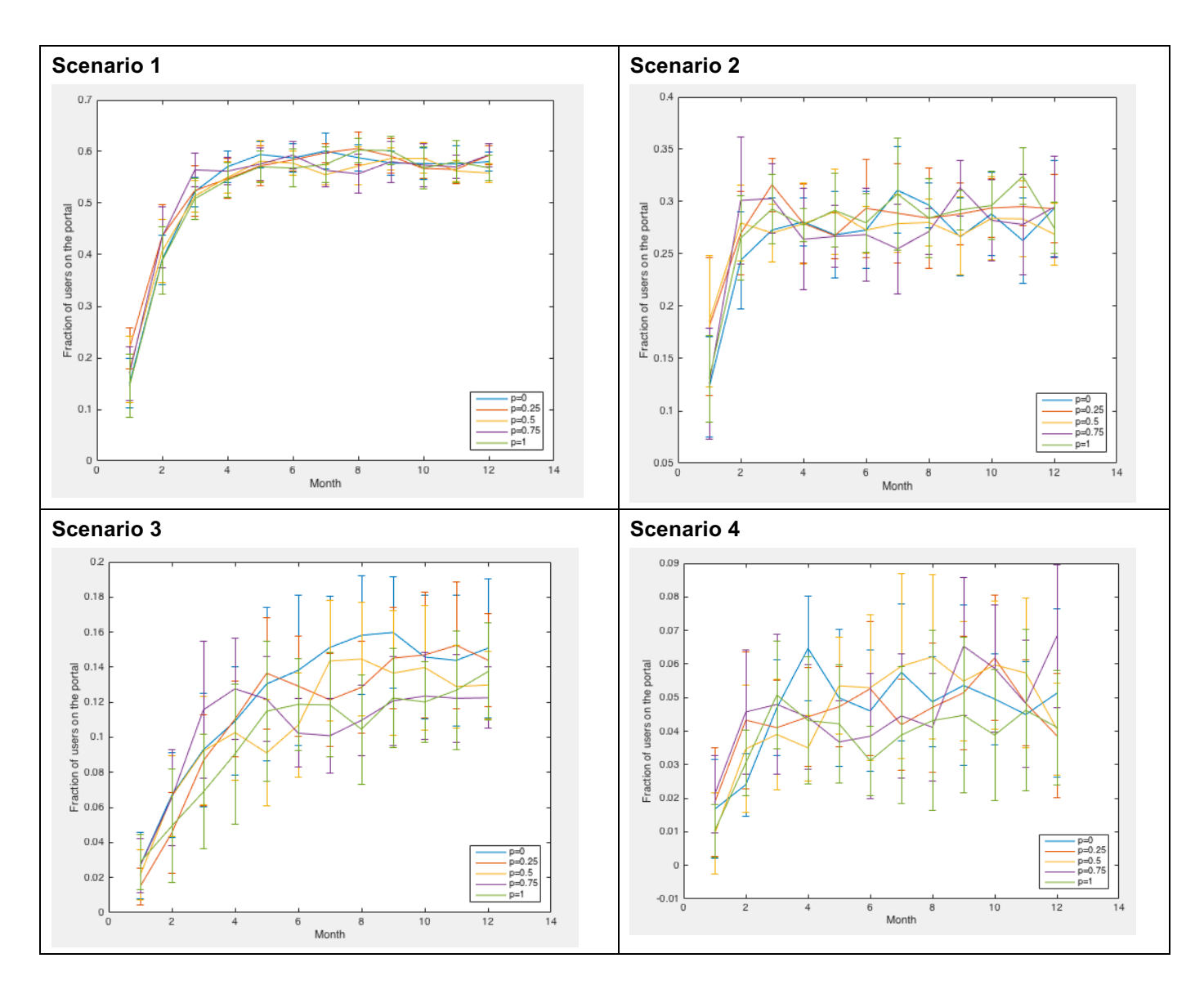


Figure 19: Trajectory of fraction of users who are adopting the portal in the four different scenarios for the case study of Terre di Pedemonte.

From the results presented in Figure 19, we see that the adoption of the portal is above 50% in Scenario 1, between 25%-30% in Scenario 2, between 10%-15% in Scenario 3, while is low (around 5%) in Scenario 1. Since at the current state of development the Young model does not influence the behaviour of the underlying portal diffusion model, varying the value of parameter p does not affect the number of portal adopters.

From the results presented in Figure 20, we remark that in all scenarios the trajectories of fraction of users who are portal adopters and have chosen behaviour E follow closely the trajectory of the fraction of users who are portal adopters.

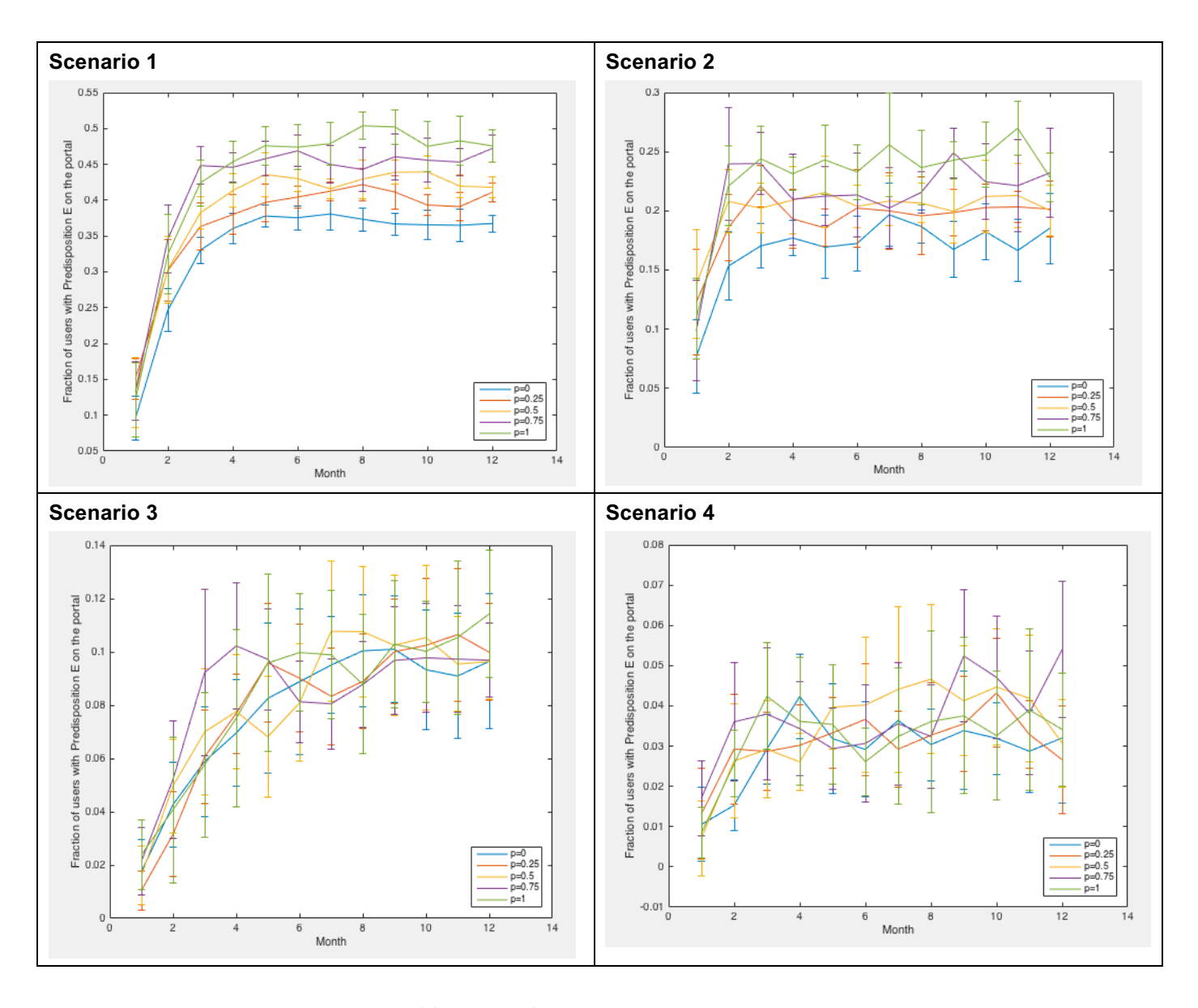


Figure 20: Trajectory of fraction of users who are on the portal and have chosen behaviour E in the four different scenarios for the case study of Terre di Pedemonte.

To assess the weight of the value of parameter p on the adoption of behaviour E, we then consider for each sub-scenario the daily fraction of the users on the portal who have chosen behaviour E. The results are summarised in Table 18.

Table 18: Average of daily fraction of portal users who have chosen behaviour E in the Terre di Pedemonte case study.

Scenario	Value of p	Fraction (%) of portal users with behaviour E
	0	63.43 (± 0.15)
4	0.25	69.29 (± 0.14)
1	0.5	74.71 (± 0.15)
	0.75	79.40 (± 0.13)
	1	83.44 (± 0.11)
	0	62.99 (± 0.23)
2	0.25	69.03 (± 0.19)
2	0.5	74.56 (± 0.20)
	0.75	79.32 (± 0.19)
	1	83.26 (± 0.13)
	0	63.76 (± 0.44)
3	0.25	69.59 (± 0.32)
3	0.5	74.79 (± 0.30)
	0.75	79.59 (± 0.56)
	1	83.12 (± 0.44)
	0	63.32 (± 0.71)
4	0.25	69.55 (± 0.90)
4	0.5	74.67 (± 0.83)
	0.75	79.50 (± 0.43)
	1	84.39 (± 0.63)

The results depicted in Table 18 show on the one hand that the fraction of portal users who have chosen behaviour E is independent of the underlying scenario, i.e. on the values of the underlying portal diffusion model. On the other hand, the results tell us that the higher the value of parameter p, the stronger the social norm - related to a respectful behaviour toward water consumption given by behaviour E - is among portal users.

To assess the influence on water consumption of the emergence of a social norm, we have thence performed 10 simulations (of one year duration: January-December) without any diffusion sub-model. The obtained daily aggregated water consumption's levels have then been compared with the daily aggregated water consumption's levels obtained in the scenarios. The results are presented in Table 19. Since the diffusion of the portal, and a fortiori the diffusion of behaviour E, is a gradual process, we have considered the consumptions during the last half of the simulation period (last 6 months).

Table 19: Influence of emergence of behaviour E among portal users on water consumption under different scenarios for the case study of Terre di Pedemonte.

Scenario	Value of p	Reduction (%) on daily consumption, last six months
	0	1.83 (± 0.57)
4	0.25	1.91 (± 0.51)
1	0.5	2.09 (± 0.58)
	0.75	2.32 (± 0.51)
	1	2.50 (± 0.53)
	0	0.90 (± 0.55)
2	0.25	0.98 (± 0.58)
2	0.5	1.01 (± 0.52)
	0.75	1.08 (± 0.54)
	1	1.12 (± 0.57)
	0	0.53 (± 0.53)
3	0.25	0.48 (± 0.57)
3	0.5	0.62 (± 0.57)
	0.75	0.54 (± 0.56)
	1	0.54 (± 0.54)
	0	0.20 (± 0.58)
4	0.25	0.12 (± 0.56)
4	0.5	0.19 (± 0.52)
	0.75	0.31 (± 0.59)
	1	0.18 (± 0.56)

From Table 19, it turns out that in scenarios where the adoption of the portal concern at least a quarter of the users (Scenarios 1 and 2), the reduction becomes measurable (around 1% or more), and reflect the strength of behaviour E as a norm among the concerned population (the higher the value of p, the higher is the reduction in the consumption). When the fraction of users who have adopted the portal is low (Scenario 3 and 4), the reduction on consumption is clearly below 1%, and the impact of the strength of behaviour E as a norm on consumption is not visible.

# 4.3.6 Modelling future behaviour under social norms: Spanish case study - EMIVASA

In this Section, we try to capture the emergence of social norms related to water consumption for the Valencia case study. For this study, the underlying social network structure is not distance based as in the previous Terre di Pedemonte case study, but it is modelled according to a scale-free network generated by the Barabasi-Albert model [Albert et al., 2002].

Scale-free networks are widely observed in social systems (see e.g. [Jackson 2008]) and the Barabasi-Albert model is one of the most studied and successful algorithm used to generate scale-free networks. The algorithm is the following. The network begins with an initial connected network of  $m_0$  nodes. New nodes are then added, one at a time, each being connected to m existing nodes, for m less or equal to  $m_0$ , with a probability proportional to the number of links that the existing nodes already have. The model thence generates a network in which most nodes have only "few" links, but also in which few nodes gradually turn into hubs (highly connected).

The Barabasi-Albert model being used is already implemented within the AnyLogic software, the only parameter for which the value has to be determined is m. Based on the empirical studies [Christakis et al., 2007, Hill et al., 2010, Salathé et al., 2010] in which the average degree k of links in social networks are found to be 6.5, we obtain the value of m for the generation of the scale-free model by using the formula m=k/2 (see e.g. [Leventhal et al., 2015]).

The robustness of the refined ABM model to the parameter *p* in the Young's diffusion model has been assessed for 2 different scenarios whose characteristics are described in Table 20.

Scenario Factor A Factor B Factor C Factor D rateAdv. | adEffect. contactRate. | infect. usePortalD. timeImmunity 1 1/month | 10% 3/week | 10% 3 months 3 weeks 2 3 month 1/month | 5% 1/week | 5% 3 weeks

Table 20: Description of the scenarios for the Valencia case study.

Scenario 1 and 2 in this case just differ on whether the values of the parameters regulating the diffusion rate in the SIRS sub-model are low or high. As before, we assume that choosing behaviour E implies a reduction of 5% in water consumption. For each scenario, we perform a sensitivity analysis with respect to parameter p in the Young model (see Section 4.2.3). We thence consider 3 sub-scenarios depending on whether the value of p is low (0), medium (0.5), or high (1). For each sub-scenario, we perform 6 runs of one year (from January 1st until end December), and consider as output (a) the number of portal users who have chosen behaviour is E, and (b) the aggregate water consumption. The results concerning the number of users who are on the portal and whose preferred behaviour is E is given in Figure 20 below, whereas in Figure 19 we report the results on the fraction of users who are adopting the portal.

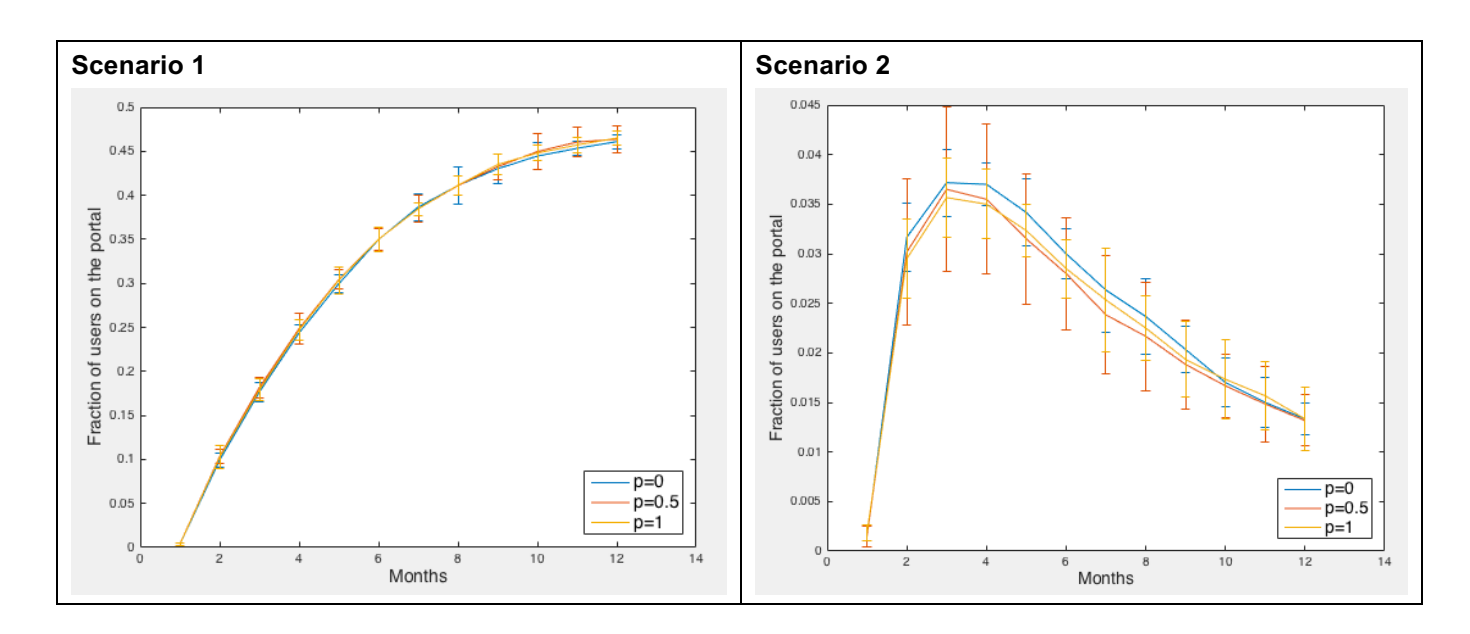


Figure 21: Trajectory of fraction of users who are adopting the portal in the two different scenarios for the case study of Valencia.

From the results presented in Figure 21, we see that the adoption of the portal is between 45-50% in Scenario 1, while it is very low (and actually decreasing) in Scenario 2. Since at the current state of development the Young model does not influence the behaviour of the underlying portal diffusion model, varying the value of parameter p does not affect the number of portal adopters.

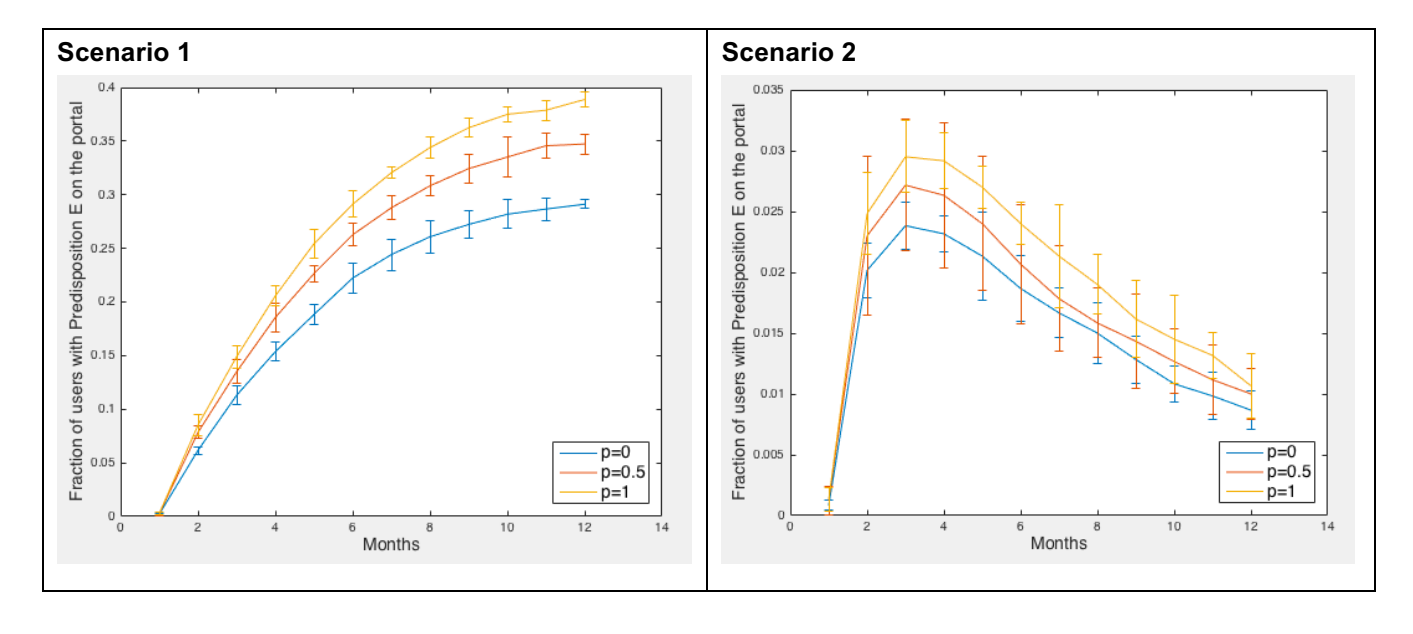


Figure 22: Trajectory of fraction of users who are on the portal and have chosen behaviour E in the two different scenarios for the case study of Valencia.

From the results presented in Figure 22, we remark that in all scenarios the trajectories of fraction of users who are portal adopters and have chosen behaviour E follow closely the trajectory of the fraction of users who are portal adopters.

To assess the weight of the value of parameter p on the adoption of behaviour E, we then consider for each sub-scenario the daily fraction of the users on the portal who have chosen behaviour E. The results are summarised in Table 21.

Table 21: Average of daily fraction of portal users who have chosen behaviour E for the Valencia case study.

Scenario	Value of p	Fraction (%) of portal users with behaviour E
	0	63.27 (± 0.65)
1	0.5	74.71 (± 0.58)
	1	83.40 (± 0.55)
	0	63.90 (± 1.68)
2	0.5	74.80 (± 1.45)
	1	83.54 (± 1.47)

The results depicted in Table 21, perfectly in line with the results presented in Table 18, corroborate once more that the fraction of portal users who have chosen behaviour E is independent of the underlying scenario and that the higher the value of parameter p, the stronger the social norm - related to a respectful behaviour toward water consumption given by behaviour E - is among portal users.

To assess the influence on water consumption of the emergence of a social norm, we have thence performed 6 simulations (of one year duration: January-December) without any diffusion sub-model. The obtained daily aggregated water consumption's levels have then been compared with the daily aggregated water consumption's levels obtained in the scenarios. The results are presented in Table 22. Since the diffusion of the portal, and a fortiori the diffusion of behaviour E, is a gradual process, we have considered the consumptions during the last half of the simulation period (last 6 months).

Table 22: Influence of emergence of behaviour E among portal users on water consumption under different scenarios for the Valencia case study.

Scenario	Value of p	Reduction (%) on daily consumption, last six months
1	0	1.42 (± 0.07)
	0.5	1.63 (± 0.10)
	1	1.88 (± 0.04)
2	0	0.11 (± 0.08)
	0.5	0.07 (± 0.03)
	1	0.15 (± 0.07)

From Table 22, it turns out that in scenarios where the adoption of the portal concern almost half of the users (Scenario 1), the reduction becomes measurable (1.4-1.9%), and reflect the strength of behaviour E as a norm among the concerned population (the higher the value of p, the higher is the reduction in the consumption). When the fraction of users who have adopted the portal is very low (Scenario 2), the reduction on consumption is insignificant, because the impact of the strength of behaviour E as a norm on consumption is not visible.

#### 4.4 Discussion and recommendation

In this Section we have described the last version of the SmartH2O agent-based model, which extends the previous simulator submitted in deliverable D3.3 and incorporates the single-user model introduced in Section 3.

The results presented in the previous sub-sections have demonstrated the effectiveness of the SmartH2O agent-based model for modelling observed consumption behaviours but also future behaviours under both price policies and the emergence of social norms concerning water consumption. The latter results were possible thanks to the introduction of two diffusion sub-models and a mechanism to capture the effect of price incentives.

Because of the limitations of the two datasets currently available, both in terms of time horizon and absence of socio-psychographic data, the current SmartH2O ABM is based only on consumption profiles coming from the single-user model. For the same reason, it was not possible to calibrate the two diffusion sub-models, and we had to rely on existing similar studies to determine the values of some of the parameters.

This notwithstanding, the underlying structure of the multi-agent model is ready. Once new data from the SES and EMIVASA users will be available, it will then be possible to calibrate the diffusion sub-models.

### Conclusions

In this deliverable we have described the final structure and configuration of the agent based model that describes the consumption behaviour of water users and their response to water saving incentives.

In Section 2, we have described the development of two novel algorithms for the disaggregation of water into end uses, the first one based on a sparse optimisation approach and the second on a hybrid signature-based iterative disaggregation approach. A first calibration and validation of the algorithms have been performed on high resolution water consumption data provided by a New Zealand study, as the SmartH2O case studies did not provide high resolution data. It has been observed that the algorithm performance drops progressively when the data sampling frequency is lower that 1 minute. Most commercial smart water meters have sampling frequencies ranging from 15 minutes to 1 hour and more. In conclusion, while these algorithms perform better than the state of the art on high frequency measures, they need to be integrated with supplemental ex-ante information on household appliances and devices to be able to provide a rough estimate of the end-use attributions.

In Section 3, we have presented the algorithm that models the water consumption behaviour of the single household. This algorithm identifies, from data, the most likely consumption profiles, it extracts the most relevant drivers associated with the above profiles, and then uses model learning to link each individual consumer to the most likely consumption profile. The model has been successfully applied to real world data both in the Swiss and in the Spanish case study. In the Swiss case, the extraction of the consumption profiles was made over the period 03/2015 – 10/2015, as the smart water meters installation was completed in February 2015. In the Spanish case study, the meters were already installed, so we were able to use a much longer training period (01/2014 -01/2016). In both cases, the validation results (on a different data set wrt the one used for the calibration) regarding the ability to describe the behaviour of a generic household were satisfactory.

Finally, in Section 4, we have described the agent based model that reproduces the adoption of the SmartH2O platform, and the subsequent response in terms of change of behaviour in water consumption. The ABM model describes the diffusion process that models the adoption of the SmartH2O platform by a fraction of the population, then it describes how the platform adopters might change their behaviour when exposed to the environmental awareness stimuli and pricing stimuli provided by the platform use. The model has been validated in both cases. It returns a slight overestimation of the average water consumption for the Swiss use case, while it performs rather well in modelling the response in the Spanish case study.

The two case studies are rather different, because of their distinct climatic and geographic conditions, but also because of the size of the samples, and the pervasiveness of the smart metering infrastructure. This asymmetry is also reflected in the calibration and validation data sets, but this also had a positive side effect, as we were able to apply to the Spanish case study the same models and data processing procedures we developed for the Swiss case study, showing their ability to scale from a database with a few hundreds of users to one with tens of thousands, which is very important for the potential future applications of the SmartH2O platform. Moreover, In the final Validation Report (Deliverable D7.3) that will be issued in March 2017 the experiments will be re-run with a larger data set in order to better appreciate the model ability to reproduce the consumer behaviour over a longer time horizon.

### 6. References

[Abed-Meraim et al, 1997] Abed-Meraim, K., Qiu, W., Hua, Y., 1997. Blind system identification. *Proceedings of the IEEE* 85, 1310–1322.

[Agudelo-Vera et al., 2014] Agudelo-Vera, C., Blokker, E., Büscher, C., Vreeburg, J., 2014. Analysing the dynamics of transitions in residential water consumption in the Netherlands. *Water Sci. Technol. Water Supply* 14, 717-727

[Albert et al., 2002] Albert R., Barabasi A.-L., 2002, Statistical mechanics of complex networks. *Rew. Mod. Phys.*, 74(1), 47-97

[Aquacraft Inc, 2011] Aquacraft Inc, 2011. Albuquerque single-family Water Use Efficiency and Retrofit Study. *Rep. Prepared for the Albuquerque Bernalillo County Water*.

[An, 2012] An, L., 2012. Modeling human decisions in coupled human and natural systems: Review of agent-based models. *Ecological modelling*.

[Armel et al., 2013] Armel, K. C., Gupta, A., Shrimali, G., Albert, A., 2013. Is disaggregation the holy grail of energy efficiency? the case of electricity. *Energy Policy* 52, 213–234.

[Athanasiadis et al., 2005] Athanasiadis, I.N., A.K. Mentes, P.A. Mitkas., and Y.A. Mylopoulos 2005. A Hybrid Agent-Based Model for Estimating Residential Water Demand. *Simulation*, 81, 3, 175-187.

[Balling et al., 2007] Balling, R.C., Gober, P., 2007. Climate variability and residential water use in the city of Phoenix, Arizona. *J. Appl. Meteorol. Climatol.* 46, 1130-1137.

[Bass, 1969] Bass, F. M., 1969. A new product growth model for consumer durables. *Management Science*, 15, 215–227.

[Batra et al., 2014] Batra, N., Kelly, J., Parson, O., Dutta, H., Knottenbelt, W., Rogers, A., Singh, A., Srivastava, M., 2014. NILMTK: An open source toolkit for non-intrusive load monitoring. arXiv preprint arXiv:1404.3878.

[Beal et al., 2014] Beal, C.D., Makki, A., Stewart, R.A., 2014. What does rebounding water use look like? an examination of post-drought and post-flood water end-use demand in Queensland, Australia. *Water Sci. Technol. Water Supply* 14, 561-568.

[Berglund, 2015] Berglund, E., 2015. Using Agent-Based Modeling for Water Resources Planning and Management. *J. Water Resour. Plann. Manage.*, 141(11)

[Balietti et al., 2011] Balietti S., Helbing D., 2011. How to Do Agent-Based Simulations in the Future: From Modeling Social Mechanisms to Emergent Phenomena and Interactive Systems Design. Santa Fe Institute Working Paper 2011-06-024. Reprinted as Chapter 2 in: Helbing D. (2012), Social Self-Organization, Understanding Complex Systems, Springer Verlag.

[Barreteau et al., 2000] Barreteau, O., Bosquet F., 2000, Shadoc: a multi-agent model to tackle viability of irrigated systems. *Ann. Operat. Res.*, 94(1-4), 139-162

[Barthelemy et al., 2001] Barthelemy, O., S. Moss, T. Downing, and J. Rouchier, 2001. Policy modelling with ABSS: The case of water demand management. Centre for Policy Modelling, Manchester Metropolitan University, Manchester, CPM Report.

[Becu et al, 2003] Becu, N., Perez, P., Walker, A., Barreteau, O., Le Page, C., 2003. Agent based simulation of a small catchment water management in northern Thailand. *Ecol.Modell.*, 170(2-3), 319-331.

[Blokker et al, 2010] Blokker, E., J. Vreeburg, and J. van Dijk, 2010. Simulating residential water demand with a stochastic end-use model. *Journal of Water Resources Planning and Management*, 136(1), 19-26.

[Borshchev et al., 2004] Borshchev, A. and Filippov, A., 2004, From Systems Dynamics and Discrete Event to Practical Agent Based Modeling: Reasons, Techniques, Tools. In: *Proceedings of the 22<sup>nd</sup> International Coneference of the System Dynamics Society*, Oxford, 25-29.

[Capasso, 2008] Capasso, V. 2008. Mathematical Structures of Epidemic Systems (2d ed.).

#### Springer

[Cardell-Oliver, 2013a] Cardell-Oliver, R., 2013. Discovering water use activities for smart metering. In: Intelligent Sensors, Sensor Networks and Information Processing, 2013 IEEE Eighth International Conference on, IEEE, 171-176.

[Cardell-Oliver, 2013b] Cardell-Oliver, R., 2013. Water use signature patterns for analyzing household consumption using medium resolution meter data. *Water Resour. Res.* 49, 8589-8599.

[Cardell-Oliver et al., 2013] Cardell-Oliver, R., Peach, G., 2013. Making sense of smart metering data. *Aust. Water Assoc. Water* J. 4, 124-128.

[Chang et al, 2014] Chang, H., Praskievicz, S-, Parandvash, H., 2014. Sensitivity of Urban Water Consumption to Wheather and Clomate Variability at Multiple temporale Scales: The Case of Portland, Oregon. *Int. J. of Geosp. And Env. Res.*, 1(1), Article 7.

[Christakis et al, 2007] Christakis, N., A., Fowler J.H., 2007. The spread of obesity in large scale network over 32 years. *N. Engl. J. Med.*, 357, 370.

Chu et al., 2009] Chu, J., C. Wang, J. Chen, and H. Wang, 2009. Agent-based residential water use behaviour simulation and policy implications: A case-study in Beijing city, *Water resources management*, 23(15): 3267-3295.

[Cominola et al, 2015a] Cominola, A., Giuliani, M., Piga, D., Castelletti, A., Rizzoli, A.E., 2015. Benefits and challenges of using smart meters for advancing residential water demand modeling and management: A review. *Environmental Modelling & Software*, vol. 72, 198-214.

[Cominola et al, 2015b] Cominola, A., Giuliani, M., Piga, D., Castelletti, A., Rizzoli, A.E., Anda, M., 2015. Modelling residential water consumers' behaviors by feature selection and feature weighting, in *Proceedings of the 36th IAHR World Congress*, The Hague (the Netherlands).

[Cominola et al, 2017] Cominola, A., Giuliani, M., Piga, D., Castelletti, A., and Rizzoli, A. E., 2017. A Hybrid Signature-based Iterative Disaggregation algorithm for Non-Intrusive Load Monitoring. *Applied Energy*, 185, 331-344.

[DeOreo et al., 1994] DeOreo, W.B., Mayer, P.W., 1994. Project Report: a Process Approach for Measuring Residential Water Use and Assessing Conservation. Technical Report.

[DeOreo et al., 1996] DeOreo, W.B., Heaney, J.P., Mayer, P.W. 1996. Flow trace analysis to assess water use. AWWA 88, 79-90.

[DeOreo et al., 2000] DeOreo, W.B., Mayer, P.W., 2000. *The End Uses of Hot Water in Single Family Homes from Flow Trace Analysis*. Seattle Public Utilities and US EPA, Seattle.

[DeOreo et al., 2011] DeOreo, W.B., Mayer, P.W., Martien, L., Hayden, M., Funk, A., Kramer-Duffield, M., Davis, R., Henderson, J., Raucher, B., Gleick, P., et al., 2011. California single-family Water Use Efficiency Study. Rep. Prepared for the California Dept. of Water Resources.

[Dong et al., 2013] Dong, M., Meira, P.C., Xu, W., Chung, C., 2013. Non-intrusive signature extraction for major residential loads. *Smart Grid, IEEE Transactions on* 4, 1421–1430.

[Downing et al., 2000] Downing, T.E., S. Moss, and C. Pahl-Wostl, 2000. Understanding Climate Policy Using Participatory Agent-Based Social Simulation. MABS, 198-213.

[Duda et al., 1973] Duda, R. O., and Hart, P. E., 1973. *Pattern classification and scene analysis*. A Wiley Interscience Publication, John Wiley and Sons, Inc.

[Edwards et al., 2005] Edwards, M., Ferrand, N., Goreaud, F., Huet, S., 2005. The relevance of aggregating a water consumption model cannot be disconnected from the choice of information avalaible on the resource. *Siml. Mode. Pratc. Theory*, 13, 287-307.

[Ernst et al., 2005] Ernst, A., C. Schulz, N. Schwarz, and S. Janisch, 2005. Shallow and deep modeling of water use in large, spatially explicit, coupled simulation system. ESSA, 158-164

[Froehlich et al., 2011] Froehlich, J., Larson, E., Saba, E., Campbell, T., Atlas, L., Fogarty, J., Patel, S., 2011. A longitudinal study of pressure sensing to infer real-world water usage events in the home. In: *Pervasive Computing*. Springer, 50-69.

[Gaiardelli, 2015] Gaiardelli, E., 2015. Development of a flexible synthetic generator of residential water consumption traces at the end-use level. Politecnico di Milano.

[Galan et al., 2009] Galan, J., A. Lopez-Paredes, and R. Del Olmo, 2009. An agent-based model for domestic water management in Valladolid metropolitan area. *Water Resources Research*, 45(5).

[Galelli et al., 2013] Galelli, S., and A. Castelletti, 2013. Assessing the predictive capability of randomized tree-based ensembles in streamflow modelling. *Hydrol. Earth Syst. Sci. Discuss.*, 10(2), 1617–1655.

[Galelli et al., 2014] Galelli, S., G. Humphrey, H. Maier, A. Castelletti, G. Dandy, and M. Gibbs, 2014. An evaluation framework for input variable selection algorithms for environmental data-driven models, *Environ. Modell. Software*, 62, 33–51.

[Giuliani et al., 2013] Giuliani, M., Castelletti, A., 2013. Assessing the value of cooperation and information exchange in large water resources systems by agent-based optimization. *Water Resour. Res.*, 49(7), 3912-3926.

[Giuliani et al, 2015] Giuliani, M., Castelletti, A., Amigoni, F., and Cai, X., 2015. Multiagent Systems and Distributed Constraint Reasoning for Regulatory Mechanism Design in Water Management. *Journal of Water Resources Planning and Management*, vol. 141, iss. 4, 2015.

[Ghahramani et al., 1997] Ghahramani, Z., Jordan, M.I., 1997. Factorial hidden markov models. Machine learning 29, 245–273.

[Gilbert , 2008] Gilbert, N., 2008. Agent-Based Models. Sage Publications, Inc.

[Griffin et al., 1991] Griffin R.C., Chang, C., 1991. Seasonality in Community Water Demand. *Eastern Journal of Agricultural Economics*. 16(2), 207-217.

[Heinrich , 2007] Heinrich, M., 2007. Water End Use and Efficiency Project (WEEP) e Final Report. BRANZ Study Report 159

[Hill et al., 2010] Hill, A.L., Rand D.G., Nowak, N.A., 2010. Infectious disease modelling of social contagion in networks. *PLoS ONE* 8, e73970.

[House-Peters et al., 2011] House-Peters, L.A., Chang, H., 2011. Urban water demand modeling: review of concepts, methods, and organizing principles. *Water Resour. Res.* 47(5)

[Young , 2003] Young, H., P., 2003, The diffusion of innovations in social network. In *The economy as an evolving complex system, vol. III*, ed. By L.E. Blume and S.N. Durlauf, Oxford University Press, 267-282

[Young, 2011] Young, H., P., 2011, The dynamics of social innovation. *Proceeding of the National Academy of Sciences*, 108 (supplement 4), 21, 285- 291.

[Jackson 2008] Jackson M.O., 2008. Social and Economic Networks. Princeton University Press

[Kenney et al., 2008] Kenney, D.S., Goemans, C., Klein, R., Lowrey, J., Reidy, K., 2008. Residential water demand management: lessons from Aurora, Colorado. *JAWRA J. Am. Water Resour. Assoc.* 44, 192-207.

[Kermack et al., 1927] Kermack, W. O., McKendrick, A. G., 1927. A Contribution to the Mathematical Theory of Epidemics. *Proceedings of the Royal Society A: Mathematical, Physical and Engineering Sciences* 115 (772), 700.

[Kermack et al, 1933] Kermack, W. O, McKendrik, A. G., 1933. A Contribution to the Mathematical Theory of Epidemics. III. Further studies of the problem of endemicity. *Proceedings of the Royal Society of London*. Series A *Mathematical, Physical and Engineering Sciences*, 141(843), 94-122.

[Kofinas et al., 2014] Kofinas, D., Mellios, N., Papageorgiou, E., Laspidou, C., 2014. Urban water demand forecasting for the island of skiathos. *Procedia Eng.* 89, 1023-1030.

[Kowalski et al., 2003] Kowalski, M., Marshallsay, D., 2003. A System for Improved Assessment of Domestic Water Use Components. *International Water Association*.

[Kwac et al., 2014] Kwac, J., Flora, J., & Rajagopal, R., 2014. Household energy consumption segmentation using hourly data. *Smart Grid, IEEE Transactions on*, *5*(1), 420-430.

[Leventhal et al., 2015] Leventhak, G.E., Hill, Al.L., Nowak, M.A., Bonhoffer S., 2015. Evolution and emergence of infectious disease in theretical and real-world networks. *Nature* 

Communications 6:6101.

[Likas et al., 2003] Likas, A., Vlassis, N., & Verbeek, J. J., 2003. The global k-means clustering algorithm. *Pattern recognition*, 36(2), 451-461.

[Loh et al., 2003] Loh, M., Coghlan, P., Australia, W., 2003. Domestic Water Use Study: in Perth, Western Australia, 1998-2001. Water Corporation.

[Lopez-Paredes et al., 2005] Lopez-Paredes, A., D. Sauri, and J.M. Galan, 2005. Urban Water management with artificial societies agents: the FIRMABAR simulator. *Simulation*, 81(3), 189-199.

[Macal et al., 2010] Macal C.M., North M.J., 2010. Tutorial on agent-based modelling and simulation. *Journal of Simulation* 4, 151-162

[Maede et al., 2006] Maede N, Islam, T., 2006. Modelling and forecasting the fiffusion of innovation, A 25-year review. *Int. Journal of Forecasting*, 22, 519-545.

[Maggioni , 2015] Maggioni, E., 2015. Water demand management in times of drought: what matters for water conservation. *Water Resour. Res.* 

[Maier et al., 2000] Maier, H. R., and Dandy, G. C., 2000. Neural networks for the prediction and forecasting of water resources variables: a review of modelling issues and applications. *Environmental modelling and software*, 15(1), 101-124.

[Maier et al., 2013] Makonin, S., Popowich, F., Bartram, L., Gill, B., Bajic, I.V., 2013. AMPds: A Public Dataset for Load Disaggregation and Eco-Feedback Research, in: *Proceedings of the 2013 IEEE Electrical Power and Energy Conference (EPEC)*.

[Matos et al., 2014] Matos, C., Teixeira, C.A., Bento, R., Varajao, J., Bentes, I., 2014. An exploratory study on the influence of socio-demographic characteristics on water end uses inside buildings. *Sci. Total Environ.* 466-474.

[Mayer et al., 1995] Mayer, P.W., DeOreo, W.B., 1995. Process Approach for Measuring Residential Water Use and Assessing Conservation Effectiveness. AWWA.

[Mayer et al., 1998] Mayer, P.W., DeOreo, W.B., 1999. *Residential End Uses of Water*. American Water Works Association.

[Mayer et al., 2004] Mayer, P.W., DeOreo, W.B., Towler, E., Martien, L., Lewis, D., 2004. Tampa water Department Residential Water Conservation Study: the Impacts of High Efficiency Plumbing Fixture Retrofits in Single-family Homes. A Report Prepared for Tampa Water Department and the United States Environmental Protection Agency.

[Mead et al., 2009] Mead, N., Aravinthan, V., 2009. Investigation of household water consumption using smart metering system. *Desalin. Water Treat.* 11, 115-123.

[Müller, 2007] Müller, M., 2007. Dynamic time warping. *Information retrieval for music and motion*, 69–84.

[Neenan et al., 2008] Neenan, B., Hemphill, R.C., 2008. Societal benefits of smart metering investments. *The electricity journal* 21, 32–45.

[Newborough et al., 1990] Newborough, M., Probert, S., 1990. Intelligent automatic electrical-load man- agement for networks of major domestic appliances. *Applied Energy* 37, 151 – 168.

[Ehart et al., 2011] N, T.L., Ehart, J., W, Cai, X., Braden, J., B., 2011, An agent based model of farmer decision-making and water quality impacts at the watershed scale under markets for carbon allowances and a second generation biofuel crop. *Water Resour. Res.*, 47(9), W09519

[Nguyen et al., 2013] Nguyen, K.A., Zhang, H., Stewart, R.A., 2013. Development of an intelligent model to categorise residential water end use events. *J. Hydro Environ. Res.* 7, 182-201.

[Nguyen et al., 2014] Nguyen, K.A., Stewart, R.A., Zhang, H., 2014. An autonomous and intelligent expert system for residential water end-use classification. *Expert Syst. Appl.* 41, 342-356.

[Olmstead et al., 2007] Olmstead, S.M., Michael Hanemann, W., Stavins, R.N., 2007. Water demand under alternative price structures. *J. Environ. Econ. Manag.* 54, 181-198.

[Piga et al., 2015] Piga, D., Cominola, A., Giuliani, M., Castelletti, A., Rizzoli, A.E., 2015. Sparse

optimization for automated energy end use disaggregation. *IEEE Transaction on Control Systems Technology*, In press.

[Polebitski et al., 2010] Polebitski, A.S., Palmer, R.N., 2010. Seasonal residential water demand forecasting for census tracts. *J. Water Resour. Plan. Manag.* 136, 27-36.

[Quinlan, 1993] Quinlan, J. R., 1993. C4. 5: programs for machine learning (Vol. 1). Morgan Kaufmann.

[Rixon et al., 2007] Rixon, A., M. Moglia, and S. Burn, 2007. Exploring Water Conservation Behaviour through Participatory Agent-Based Modelling. In: Andrea Castelletti, Rodolfo Soncini-Sessa (ed.). *Topics on System Analysis and Integrated Water Resources Management*, Elsevier, 73-96.

[Roberts , 2005] Roberts, P., 2005. Yarra Valley Water: 2004 Residential End Use Measurement Study. Technical Report. Yarra Valley Water Melbourne. Melbourne, Australia.

[Romano et al., 2014] Romano, G., Salvati, N., Guerrini, A., 2014. Estimating the determinants of resi- dential water demand in Italy. *Water* 6, 2929-2945.

[Rosenberg, 2010] Rosenberg, D., 2010. Residential water demand under alternative rate structures: simulation approach. *J. Water Resour. Plan. Manag.* 136, 395-402.

[Ruzzelli et al., 2010] Ruzzelli, A.G., Nicolas, C., Schoofs, A., O'Hare, G.M., 2010. Real-time recogni- tion and profiling of appliances through a single electricity sensor, in: Sensor Mesh and Ad Hoc Communications and Networks (SECON), 2010 7th Annual IEEE Communications Society Conference on, IEEE. 1–9.

[Salathé et al., 2010] Salathé, M., et al., 2010. A high resolution human contact network for infectious disease transmission. *Proc. Natl Acad. Sci. USA* 107, 22020-22025

[Sakoe et al., 1978] Sakoe, H., Chiba, S., 1978. Dynamic programming algorithm optimization for spoken word recognition. Acoustics, Speech and Signal Processing, *IEEE Transactions on* 26, 43–49.

[Schluter et al., 2007] Schluter, M. and Pahl-Wostl, C., 2007, Mechanisms of resilience in common-pool resource management systems: an agent based model of water use in a river basin. *Ecol. Soc.*, 12(2).

[SDU, 2011] SDU, 2011. Urban Water Management Plan 2010. Technical Report. City of Sacramento, Sacramento, California.

[SJESD, 2011] SJESD, 2011. Urban Water Management Plan. Technical Report. City of San Jose, Sacramento, California.

[Sycara, 1998] Sycara, K.P., 1998. Multiagent systems. Al Magazine, 19(2), 79-92.

[Shoham et al., 2008] Shoham, Y., Leyton-Brown, K., 2008. *Multiagent Systems*. Cambridge University Press.

[Tsegaye eta I., 2009] Tsegaye, S., and K. Vairavamoorthy, 2009. Agent-Based Modeling to Estimate Residential Water Demand and to Explore Optimal Demand Side Water Management strategies. SWITCH Project Report.

[Willis et al., 2009a] Willis, R.M., Stewart, R.A., Capati, B., 2009. Closing the loop on water planning: an integrated smart metering and web-based knowledge management system approach. In: *ICA* 2009, International Water Association.

[Willis et al., 2009b] Willis, R., Stewart, R.A., Panuwatwanich, K., Capati, B., Giurco, D., 2009. Gold coast domestic water end use study. *Water* 36, 79-85.

[Willis et al., 2011] Willis, R.M., Stewart, R.A., Panuwatwanich, K., Williams, P.R., Hollingsworth, A.L., 2011. Quantifying the influence of environmental and water conservation attitudes on household end use water consumption. *J. Environ. Manag.* 92, 1996-2009.

[Wooldridge, 2002] Wooldridge M., 2002. *An introduction to multiagent system*. Wiley, Hoboken, NJ.

[Yang et al., 2009] Yang, Y.-C. E., Cai, X., Stipanovic, D.M., 2009. A decentralized optimization algorithm for multiagent system-based watershed management. *Water Resour. Res.*, 45(8), W08430

[Zoha et al., 2012] Zoha, A., Gluhak, A., Imran, M.A., Rajasegarar, S., 2012. Non-intrusive load monitoring approaches for disaggregated energy sensing: A survey. *Sensors* 12, 16838–16866.

# Appendix: Model engineering

In this appendix we briefly describe the engineering setup of the agent based simulation model.

The dataset read by the simulator is provided as excel files. The files are populated by data mining processes executed by the researchers that developed the classifier. The referring use case has been described in the D2.3 Functional specifications, 10.1.1 – Context.

At the current state of development, the simulator is a Java applet that is able to read the excel files, load the data into its memory structures, and log the runtime execution messages to a log file in the file system. There is no analytical output: all the information is shown in charts and diagrams on the simulation window.

In order to engineer the ABM model to be capable to read data directly from the smart meter monitoring system, we need to add some external modules to the actual simulator applet.

Due to the fact that the simulator, as a Java applet, is driven by strong security design that makes it unable to communicate easily outside its process and memory space, we are going to develop external modules. With the modules design we'll be able to build the dataset, export it to excel files, and eventually leave the model read and use that data as usual.

#### **Modules interaction**

The UML diagram depicted in Figure 23 below describes how the modules are interacting.

The Simulator requests to update and classify the dataset. The Loader module downloads the data and pre-processes them for the classifier module. The classifier is then able to train, determine and validate the classification. Eventually, the data produced by the classifier are read by the Simulator. Based on that the new model is generated and simulations are performed.

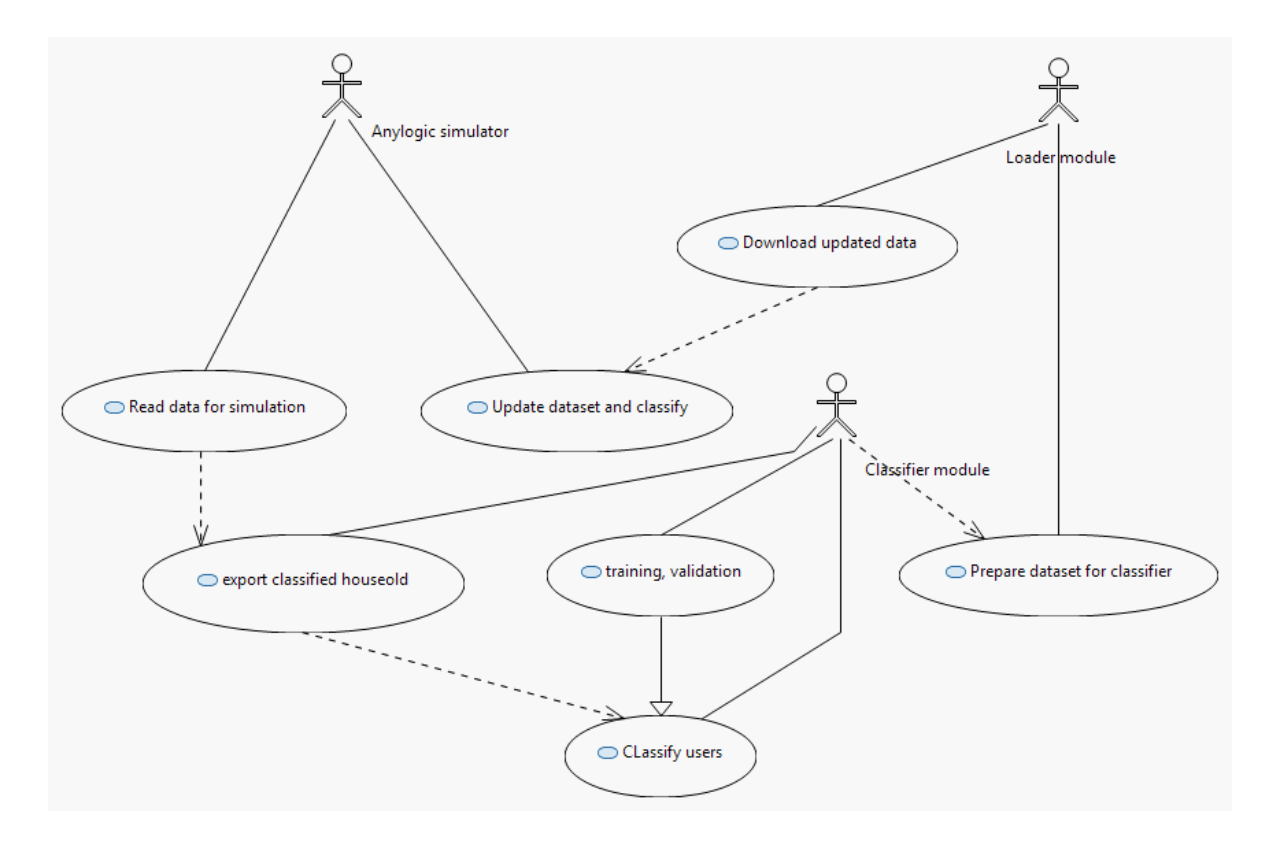


Figure 23: UML diagram of the interactions between modules.

## The logic of modules interaction

The UML sequence diagram presented in Figure 24 shows when the modules interact with each other.

The simulator requests to update and classify data. The loader process is spawned and it downloads data from the database. When it finishes updating the dataset, the latter is saved to the file system. A request for classifying the data is raised. The classifier module process starts. It loads the dataset prepared by the loader. Then, it either only classifies, or it also performs both the training and validation actions. When the aforementioned actions have been performed, the classified dataset is written to the file system. Finally, a message with the result code of the whole operation is sent back to the Loader.

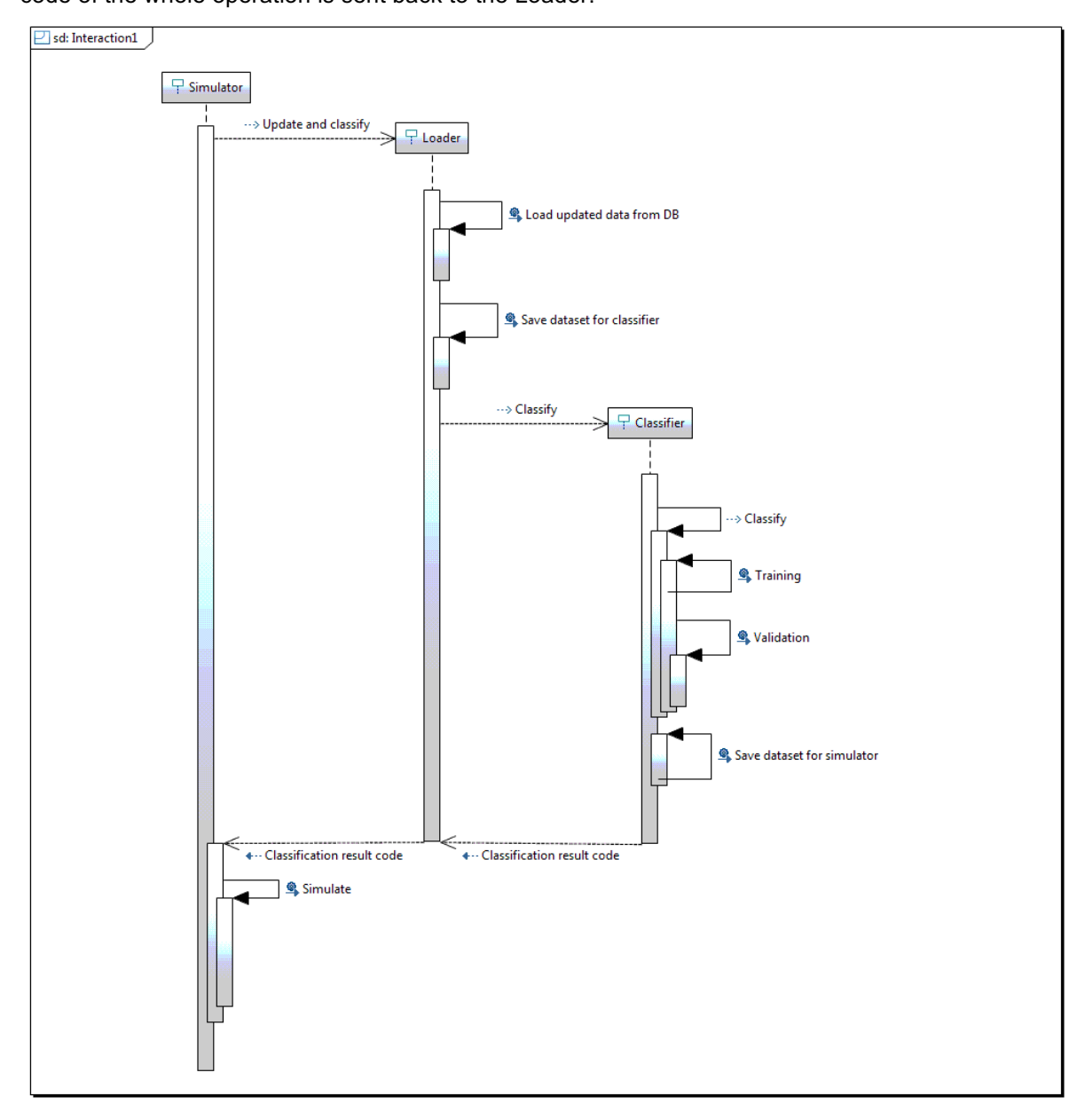


Figure 24: UML sequence diagram of the logic of interaction among modules.

The loader sends back the result code to the Simulator. The Simulator can finally run the simulation based on the new dataset.

## Deployment of the modules

The UML deploy diagram depicted in Figure 25 illustrates the deployment on the utility computer. We assume that the utility PC is a Windows® operating system.

The Simulator runs in the Java Virtual Machine executed by the applet. The loader is a python module, and the Classifier is a win32 executable. At the current state, we are not sure if the Classifier will remain win32 or it will be translated to a portable runtime like python.

In order to allow to the Loader to communicate with the database, a VPN module could be deployed. At the current state of development, the database is read accessing the remote DB machine throughout its firewall, properly setup on a list of allowed external IPs.

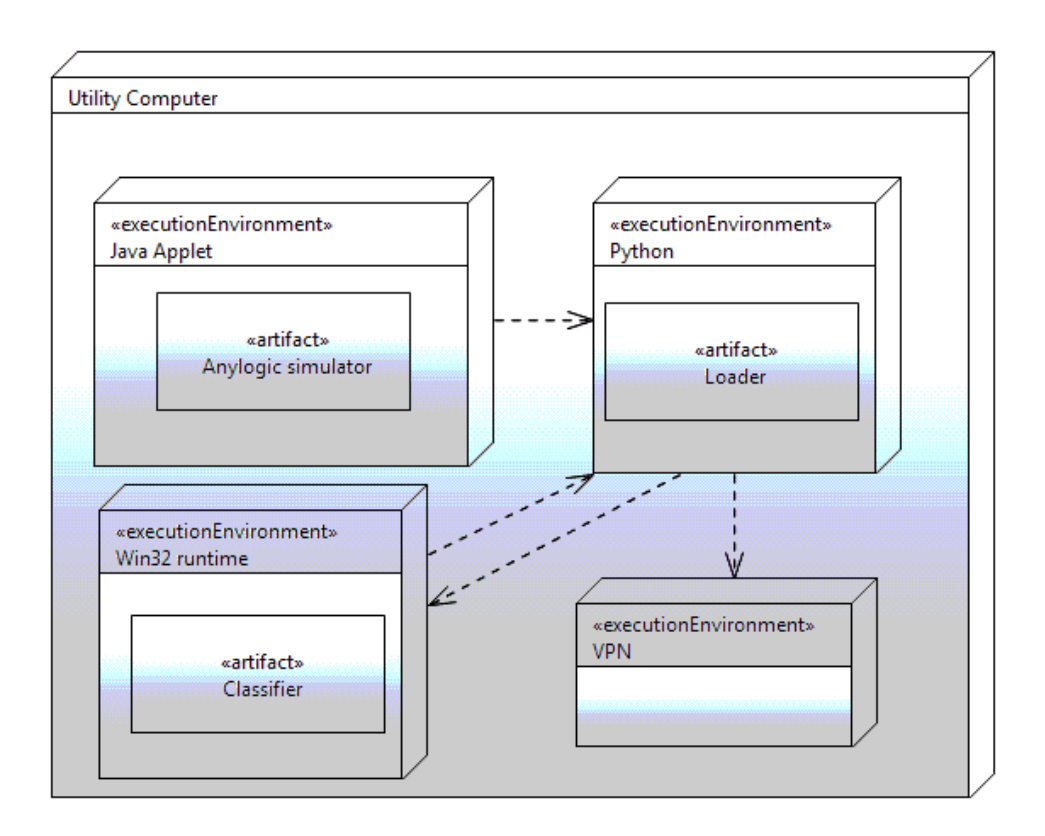


Figure 25: UML deploy diagram.